HHS Public Access

Author manuscript

Cell Rep. Author manuscript; available in PMC 2021 September 06.

Published in final edited form as:

Cell Rep. 2021 August 24; 36(8): 109613. doi:10.1016/j.celrep.2021.109613.

Pro-inflammatory β cell small extracellular vesicles induce β cell failure through activation of the CXCL10/CXCR3 axis in diabetes

Naureen Javeed[1,3,*], **Tracy K. Her**[1], **Matthew R. Brown**[1], **Patrick Vanderboom**[2], **Kuntol Rakshit**[1], **Aoife M. Egan**[2], **Adrian Vella**[2], **Ian Lanza**[2], **Aleksey V. Matveyenko**[1,2]

[1]Department of Physiology and Biomedical Engineering, Mayo Clinic, Rochester, MN 55905, USA

[2]Division of Endocrinology, Diabetes, and Metabolism, Mayo Clinic, Rochester, MN 55905, USA

[3]Lead contact

SUMMARY

Coordinated communication among pancreatic islet cells is necessary for maintenance of glucose homeostasis. In diabetes, chronic exposure to pro-inflammatory cytokines has been shown to perturb β cell communication and function. Compelling evidence has implicated extracellular vesicles (EVs) in modulating physiological and pathological responses to β cell stress. We report that pro-inflammatory β cell small EVs (cytokine-exposed EVs [cytoEVs]) induce β cell dysfunction, promote a pro-inflammatory islet transcriptome, and enhance recruitment of $CD8^+$ T cells and macrophages. Proteomic analysis of cytoEVs shows enrichment of the chemokine CXCL10, with surface topological analysis depicting CXCL10 as membrane bound on cytoEVs to facilitate direct binding to CXCR3 receptors on the surface of β cells. CXCR3 receptor inhibition reduced CXCL10-cytoEV binding and attenuated β cell dysfunction, inflammatory gene expression, and leukocyte recruitment to islets. This work implies a significant role of pro-inflammatory β cell-derived small EVs in modulating β cell function, global gene expression, and antigen presentation through activation of the CXCL10/CXCR3 axis.

Graphical Abstract

*Correspondence: javeed.naureen@mayo.edu.

AUTHOR CONTRIBUTIONS

N.J. and A.V.M. designed the research. N.J., T.K.H., P.V., and K.R. performed experiments. N.J., P.V., M.R.B., and K.R. analyzed data. A.M.E., A.V., I.L., and A.V. offered technical advice. N.J. and A.V.M. wrote the manuscript, and all authors reviewed the manuscript.

SUPPLEMENTAL INFORMATION

Supplemental information can be found online at https://doi.org/10.1016/j.celrep.2021.109613.

DECLARATION OF INTERESTS

The authors declare no competing interests.

INCLUSION AND DIVERSITY

One or more of the authors of this paper self-identifies as an underrepresented ethnic minority in science.

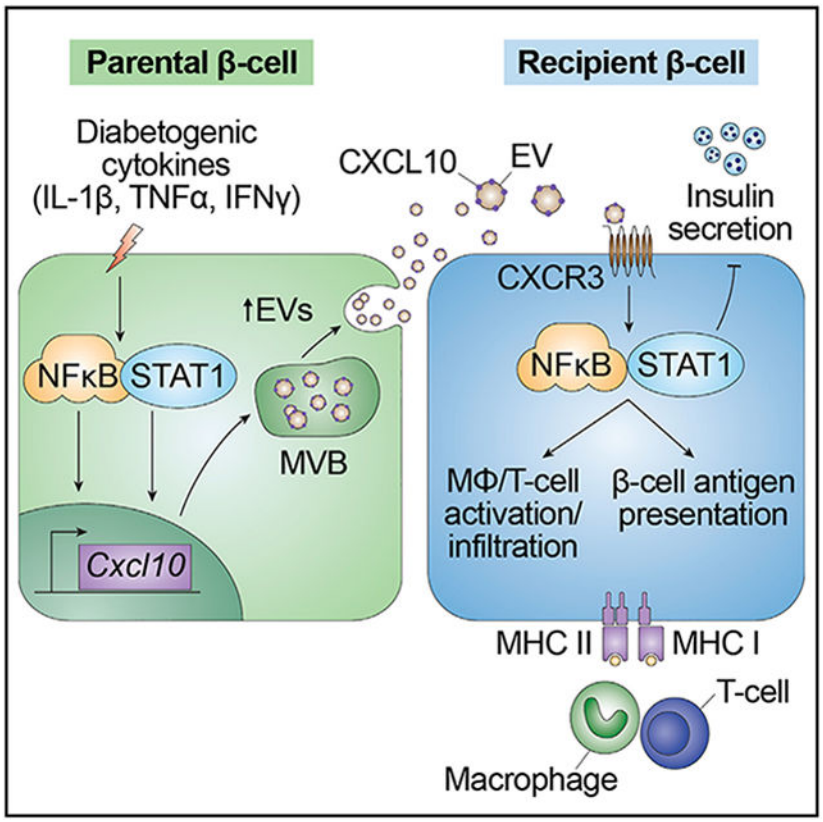

In brief

Javeed et al. demonstrate the importance of pro-inflammatory-exposed β cell-derived extracellular vesicles (cytoEVs) as facilitators of β cell dysfunction and a pro-inflammatory islet microenvironment. Physiological and mechanistic evidence implicates CXCL10/CXCR3 axis activation mediated by cytoEVs and improvements in β cell function upon CXCR3 receptor blockade.

INTRODUCTION

The pathophysiology of diabetes mellitus is complex, with evidence suggesting that loss of functional β cell mass is a hallmark abnormality responsible for induction of hyperglycemia (Matveyenko and Butler, 2008). Loss of functional β cell mass mediated by autoimmune destruction in type 1 diabetes (T1D) or exposure to pro-diabetogenic factors such as systemic inflammation in T1D and type 2 diabetes (T2D) has been shown to contribute to a compromised insulin secretory response through loss of insulin synthesis and secretion (Kahn et al., 2009; Sherry et al., 2005; Sims et al., 2020), β cell numbers (Butler et al., 2003; Meier et al., 2005), and dedifferentiation (Moin and Butler, 2019). Specifically, exposure to key pro-inflammatory cytokines (e.g., interleukin-1β [IL-1β], tumor necrosis factor alpha [TNF-α], and interferon γ [IFNγ]) has been shown to recapitulate several aspects of β cell functional failure observed during induction and progression of diabetes (Donath et al.,

2003; Eizirik et al., 2009). However, the mechanisms by which pro-inflammatory cytokines mediate deleterious effects on β cells remain under investigation.

Recent studies have implicated small circulating cell membrane-derived vesicles called extracellular vesicles (EVs) in the homeostatic process through delivery of bioactive cargoes locally and systemically to neighboring cells/tissues (Mathivanan et al., 2010). EV content is often reflective of the cell of origin and the physiological state of the cell (i.e., disease onset, cellular stressors) and can include various DNAs, RNAs, cell surface and cytosolic proteins, and lipids (Javeed, 2019; Kalluri and LeBleu, 2020). Exact classification of EV subtypes is an ongoing process because of inherent EV heterogeneity and, thus, a lack of consensus for specific markers that distinguish major EV subtypes: (1) ectosomes (i.e., microparticles, microvesicles, ~50–1 000 nm in size), which shed from the plasma membrane, and (2) exosomes (~30–150 nm), which are derived from endosome compartments (Théry et al., 2018). Unless the method of biogenesis has been established, the term “EV” in conjunction with the size of the vesicle (i.e., small EVs, <200 nm; medium/large EVs, >200 nm), density, or origin of the EVs, is used to describe EV subpopulations (Théry et al., 2018).

Recent evidence has implicated β cell-derived EVs in modulating physiological and pathological responses to β cell stress and inflammation (Guay et al., 2015; Palmisano et al., 2012; Sheng et al., 2011). Pro-inflammatory cytokine exposure to β cells has been shown to enhance packaging of the immunostimulatory endoplasmic reticulum (ER) chaperone proteins calreticulin, Gp96, and ORP150 (Cianciaruso et al., 2017) and the inflammation-associated proteins TNFR1 and ICAM-1 (Palmisano et al., 2012) into β cell EVs in addition to pro-apoptotic microRNAs (miRNAs) (Guay et al., 2015; Lakhter et al., 2018). Moreover, a growing number of publications have implicated β cell-derived EVs in immunomodulation of various lymphocytic populations (Bashratyan et al., 2013; Rutman et al., 2018; Sheng et al., 2011). For example, β cell EVs (specifically exosomes) have been found to activate antigen-presenting cells (APCs) and enhance T cell proliferation in the non-obese diabetic (NOD) mouse model of T1D (Sheng et al., 2011). Moreover, studies have also identified β cell auto-antigens in β cell-derived EVs from cell culture and from mouse and human islets (Cianciaruso et al., 2017; Hasilo et al., 2017; Tesovnik et al., 2020). However, what remains to be fully deduced is the effect and underlying mechanisms pro-inflammatory β cell EVs exert on β cell function, global gene expression, and islet immune cell recruitment.

In this work, we focused on the small EV subtype secreted from β cells in response to key diabetogenic pro-inflammatory cytokines (cytokine-exposed EVs [cytoEVs]). We found that cytoEVs alter β cell function and the islet transcriptome and promote an inflammatory islet microenvironment. This was mediated through enrichment of the chemokine CXCL10 in cytoEVs and its subsequent targeting to recipient β cells because inhibition of the CXCL10/CXCR3 axis enhanced β cell functionality and reduced transcriptional activation of the key pro-inflammatory mediators nuclear factor κB (NF-κB) and STAT1. Moreover, we implicated the immunogenicity of cytoEVs through identification of enriched gene transcripts associated with antigen processing and presentation and enhanced migration of cytotoxic $CD8^+$ T lymphocytes and macrophages in islets exposed to cytoEVs.

RESULTS

Isolation and characterization of cell line-derived β cell small EVs

For isolation of β cell-derived EVs, MIN6 cells were exposed to a combination of key diabetogenic pro-inflammatory cytokines (cytomix [CYTO], IL-1β [0.2 ng/mL], TNF-α [10 ng/mL], and IFNγ [10 ng/mL]) for 48 h (Nunemaker, 2016). Because of reported heterogeneity of EV subpopulations, our focus was on the small EV subtype, and therefore careful consideration was taken to characterize this population of EVs under normal physiological and pathological conditions (i.e., with or without pro-inflammatory cytokines). The small EV population was isolated from the conditioned medium using differential ultracentrifugation (Figure 1A; Javeed et al., 2015). Upon small EV isolation, control EVs (ctlEVs) and pro-inflammatory cytokine-exposed EV (cytoEV) fractions were subjected to western blot analysis of common small EV markers of endosome origin (i.e., exosomes), including TSG101, CD9, and ALIX (Figure 1B; Théry et al., 2018). In addition to the presence of these small EV markers in ctlEV and cytoEV fractions, transmission electron microscopy (TEM) revealed intact vesicles in the range of small EVs (~100 nm; Figure 1C). Furthermore, ctlEVs were dyed with a red lipophilic membrane dye, and EV internalization was shown to occur within an hour of small EV addition to mouse islets (Figure 1D).

Studies have reported increases in EV production and secretion during the pathogenesis of diabetes (Eguchi et al., 2016; Freeman et al., 2018). Thus, we next set out to assess whether diabetogenic pro-inflammatory cytokines themselves augment β cell EV production/secretion. Nanoparticle tracking analysis (NTA) assessment of ctlEV versus cytoEV fractions revealed an ~2-fold increase in particle concentration and an ~50% reduction in the average modal size of cytoEVs versus ctlEVs (Figure 1E). These results suggest a propensity for augmented release of small EVs under pro-inflammatory stress.

Pro-inflammatory β cell small EVs promote β cell dysfunction in islets

To assess whether increased cytokine-mediated production and secretion of small EVs contributes to β cell functional decline, we first assessed glucose-stimulated insulin secretion (GSIS) in isolated C57BL/6L mouse islets exposed to pro-inflammatory cytokines in the presence or absence of the neutral sphingomyelinease inhibitor GW4869, which irreversibly blocks ceramide-mediated inward reverse budding in multivesicular bodies, restricting formation of small EVs of endosomal origin (Figure 2A; Essandoh et al., 2015). Consistent with previous work, exposure of mouse islets to CYTO resulted in complete loss of GSIS response, characterized by an ~90% reduction in insulin stimulation index versus untreated islets (Figure 2B). Impressively, inhibition of endosome-derived small EV secretion with GW4869 partially restored the GSIS response in CYTO-treated isolated islets (~7-fold increase in GSIS, $p < 0.05$ versus CYTO; Figure 2B). To confirm the efficacy of the GW4869 compound, protein expression of the common EV biogenesis markers CD63, ALIX, and RAB7 in MIN6 cells was elevated with addition of CYTO and reduced notably upon addition of GW4869 (Figure 2C; quantitative assessment of 3–4 blots shown in Figure S1A).

Next, we sought to elucidate whether cytoEVs alone can recapitulate the deleterious effects of pro-inflammatory cytokines on β cell function and turnover in isolated C57BL/6L mouse islets (Figures 2D-2H). Exposure of islets to cytoEVs alone significantly diminished the GSIS response, characterized by an ~75% reduction in insulin stimulation index, whereas no significant changes were observed in GSIS with ctlEV addition (Figure 2E). To confirm that the observed β cell dysfunction can be solely attributed to cytoEVs and not additional secreted factors in the conditioned medium, islets exposed to conditioned medium devoid of cytoEVs showed no alterations in GSIS (Figure 2F). Furthermore, exposure of islets to cytoEVs did not alter the frequency of β cell apoptosis or proliferation, as indicated by quantification of $TUNEL^+$ and $Ki67^+$ β cells in isolated islets ($p > 0.05$ versus ctlEVs; Figures 2G and 2H), nor were β cell numbers affected (quantified as average $insulin^+$ area/islet; Figure S1B). These data suggest that increased secretion of β cell-derived small EVs contributes to induction of cytokine-mediated β cell dysfunction without altering β cell apoptosis and/or proliferation.

Pro-inflammatory β cell small EVs promote distinct transcriptional alterations in islets

As we found that cytoEVs induce β cell dysfunction in isolated islets, we next set out to gain insights into the mechanisms underlying this effect by examining global gene expression in islets exposed to cytoEVs using RNA sequencing. Our analysis revealed ~580 unique genes that were upregulated significantly with cytoEV addition and ~670 genes that were downregulated ($p < 0.05$ and fold change [FC] ≥ 1.5; Figure 3A). Next we used rank-rank hypergeometric analysis (RRHO) (Plaisier et al., 2010) to compare the transcriptome of islets exposed to cytoEVs with an existing database of transcriptomes of β cells from T1D donors (n = 4, GSE121863) (Russell et al., 2019). Factoring in cross-species comparison, the results show a striking similarity between cytoEV-exposed mouse islets and human T1D β cell transcriptomes, as evidenced by overlap of upregulated genes from both datasets ($p < 1 \times 10^{-50}$), depicted in the upper right quadrant (Figure 3B). The topmost upregulated transcripts upon cytoEV addition to islets included several chemokines, such as CXCL9 (2.6-fold), CXCL10 (2.7-fold), and CXCL11 (1.6-fold), consistent with transcripts upregulated in T1D β cells (Figures 3A and 3C). Moreover, pathway analysis (Kyoto Encyclopedia of Genes and Genomes [KEGG]) depicted a significant enrichment of genes belonging to several inflammation-associated pathways, such as antigen processing and presentation (mmu04612), chemokine signaling (mmu04062), and the NF-κB pathway (mmu04064) with cytoEV addition (Figure 3D). *In silico* modeling of cytoEV-enriched KEGG pathways revealed significantly correlated pathways relating to chemokine signaling, inflammation, and antigen presentation (Figure 3E; $p < 0.05$). Of interest was enrichment of the chemokine signaling pathway, which we confirmed by performing gene set enrichment analysis (GSEA) on a subset of key genes regulating CXCR3 signaling; we found that enrichment of this pathway was driven in part by significant upregulation of the noted chemokines CXCL9, CXCL10, and CXCL11 (false discovery rate [FDR] < 0.001; Figure 3F). These observations were also confirmed at the protein level by demonstrating robust upregulation of CXCL10 protein expression in isolated islets exposed to cytoEVs (Figure S2A). Consistently, increased β cell CXCL10 protein expression was also confirmed in mouse models of T1D, including the NOD (Figure S2B) and multiple low-dose streptozotocin (MLD-STZ) models (Figure S2C).

To gain further insights into cytoEV-mediated transcriptional alterations, we performed *de novo* motif analysis to identify enriched transcription factor binding sites within promoter regions of islet genes upregulated upon cytoEV treatment (Figure 3G). The results revealed the topmost significantly enriched transcription factor motif to be for IFN regulatory factors (IRFs) that are associated with IRF1–IRF4, STAT1, and IFN-sensitive response element (ISRE); for example, along with the NF-κB-associated transcription factor motif (Figure 3G). Interestingly, the NF-κB (Burke et al., 2015) and JAK/STAT (Burke et al., 2016) pathways lie downstream of CXCR3 signaling and are associated with β cell failure in T1D and T2D. Consistently, GSEA showed significant enrichment for key genes regulating both of these pro-inflammatory pathways in islets exposed to cytoEVs (Figure 3H). Moreover, immunofluorescence staining of islets exposed to cytoEVs revealed further evidence of robust NF-κB and STAT1 pathway activation, as shown by marked upregulation of phosphorylated p65 and STAT1 in β cells (Figures 3I and 3J).

Proteomic analysis of pro-inflammatory β cell small EV content reveals a distinct protein signature

As we have shown so far, cytoEVs exert detrimental effects on islets through a reciprocal relationship between alterations in β cell function and activation of inflammation-associated pathways. Next we sought to examine the protein content of cytoEVs (versus ctlEVs) to determine inflammation-mediated alterations in β cell small EV protein cargo. Proteomic analysis identified over 70 differentially expressed proteins between ctlEVs and cytoEVs, of which 39 proteins were uniquely enriched and 33 proteins were downregulated in cytoEVs (versus ctlEVs; Log_2 [FC] > 1; Figures 4A and S3). The chemokines CXCL9 and CXCL10 were identified as two highly expressed and uniquely enriched proteins in cytoEVs (Figure 4B; ~40 fold each versus ctlEVs). Consistently, pathway analysis (Gene Ontology [GO]) of proteins enriched in cytoEVs revealed upregulation of pathways most associated with the immune system process (GO: 0002376), which showed the presence of CXCL9 and CXCL10 (Figure 4C). Moreover, additional proteins significantly enriched in cytoEVs include major histocompatibility complex (MHC) class I molecules (i.e., H2-Q8, H2-D1, and H2-K1) and Gbp families of IFN-inducible GTPases (i.e. GBP-2 and GBP4; Figure 4C). Last, we performed protein expression validation of CXCL10 in cytoEVs by demonstrating complete absence of the chemokine in ctlEVs and conditioned medium devoid of EVs through western blot analysis (Figure 4D) and ELISA (Figure S4). These data suggest that the proteome of cytoEVs is highly altered to favor a “pro-inflammatory profile,” which includes significant enrichment of the Th1 chemokines CXCL9 and CXCL10 along with MHC class I molecules.

Pro-inflammatory β cell small EVs activate the CXCL10/CXCR3 axis in β cells

We next sought to discern the topology of CXCL10 in cytoEVs to determine their exact mechanism of CXCR3 pathway activation in β cells. Reports have shown that many cytosolic proteins are membrane bound rather than contained within EVs, and this conformation helps to facilitate direct binding of the EV surface-bound protein to cell surface receptors (Cvjetkovic et al., 2016; Javeed, 2019). To assess whether CXCL10 in cytoEVs is membrane bound, isolated cytoEVs were treated with proteinase K (PK) to remove surface-bound proteins (Cvjetkovic et al., 2016). Western blot analysis showed a

complete absence of CXCL10 with PK treatment, along with GAPDH, a common surface-bound EV protein. In contrast, TSG101 (a known intraluminal EV protein) remained intact in cytoEVs despite PK addition (Figure 4E; Cvjetkovic et al., 2016).

Next, to assess the binding ability of surface-bound CXCL10 in cytoEVs to β cell CXCR3 receptors, we utilized a proximity ligation assay (PLA) to detect endogenous protein-protein interactions *in situ*, as utilized previously in β cells (Javeed et al., 2015; Pearson and Soleimanpour, 2019). Isolated mouse islets were treated with their respective conditions (Figure 5A) and then dispersed into single-islet cells for ease of identification (Javeed et al., 2015; Pearson and Soleimanpour, 2019) of β cells through immunofluorescence staining. Primary antibodies for the ligand (CXCL10) and the receptor (CXCR3) were combined with fluorescently labeled secondary PLA probes. When the probes are in close proximity, a hybridizing connector oligo joins the probes, allowing amplification of the signal, which manifests as a punctate fluorescent dot. As expected, addition of CYTO to islets increased CXCL10/CXCR3 interactions within β cells (versus untreated, −EVs), as indicated by an increase in green PLA punctate dots (~2.8-fold; Figures 5A-5C). Interestingly, cytoEV addition alone displayed a similar increase in CXCL10/CXCR3 interactions, suggesting that the abundance of surface-bound CXCL10 on cytoEVs binds directly to and activates CXCR3 receptors on the surface of β cells (~3.8-fold; Figures 5A-5C). Furthermore, CXCL10 antibody neutralization on cytoEVs reduced the number of PLA interactions (~50%), whereas blockade of the CXCR3 receptor with the compound AMG487 (Wang et al., 2019) reduced CXCL10/CXCR3 interactions even further (~75% reduction; Figures 5A-5C).

CXCR3 receptor blockade attenuates deleterious effects of pro-inflammatory β cell small EVs in islets

As CXCR3 receptor antagonism was found to significantly reduce CXCL10-cytoEV:CXCR3 interactions, we next assessed the efficacy of AMG487 on cytoEV-mediated β cell dysfunction and gene expression. We found that CXCR3 receptor inhibition in the presence of cytoEVs displayed marked restoration of islet GSIS (versus cytoEV treatment alone), as evidenced by partial restoration of the insulin stimulation index (~2.3-fold increase; Figures 5D and 5E). Consistently, mRNA expression of β cell identity markers such as *Ins*, *Pdx1*, and *Nkx6.1* was decreased significantly with cytoEV addition to islets, whereas AMG487 restored endogenous transcript levels (Figure 5F). Transcripts associated with the CXCL10/CXCR3 axis and downstream pathways such as NF-κB and STAT1 (i.e., *Cxcl10*, *Nfκb1*, and *Stat1*) were elevated significantly with cytoEV addition, whereas addition of AMG487 reduced expression of each inflammatory transcript (Figure 5F).

Pro-inflammatory β cell small EVs enhance antigen presentation and immune cell recruitment in islets

Recent evidence suggests that β cells themselves have the capacity to upregulate MHC class I for recruitment of cytotoxic $CD8^+$ T cells (Hamilton-Williams et al., 2003) and MHC class II for $CD4^+$ T cells (Zhao et al., 2015) following exposure to pro-inflammatory cytokines. RNA sequencing (RNA-seq) data from cytoEV-treated islets indicates the topmost enriched KEGG pathway to be antigen processing and presentation (mmu0412;

Figure 3D). Interestingly, cytoEV-enriched transcripts in islets include (1) transporters associated with antigen processing (Tap1/2) and β2-microglobulin (B2m), (2) several MHC class I (H2-K1 and H2-D1) and MHC class I-related genes (H2-Qs), and (3) the MHC class II transactivator *Ciita*, which is critical for $CD4^+$ T cell recruitment to islets (Figure 6A; Devaiah and Singer, 2013). Therefore, we wanted to first assess the migratory capacity of $CD8^+$ cytotoxic T cells as well as bone marrow-derived macrophages (BMDM) in isolated islets treated with cytoEVs using a chemotaxis assay. The results depicted a marked elevation in $CD8^+$ T cell and BMDM migration to the cytoEV "primed" islets (represented in relative fluorescence units [RFUs], ~4-fold and ~28-fold, respectively; Figures 6B and 6C). Consistently, blockade of the CXCR3 pathway with AMG487 significantly reduced cytotoxic $CD8^+$ lymphocyte and BMDM migration in response to cytoEV treatment (Figures 6B and 6C). Lastly, we also confirmed a significant increase in MHC class I and II expression in $insulin^+$ (2.4-fold and 2.6-fold, respectively; $p < 0.05$) and $glucagon^+$ (1.5-fold and 1.7-fold, respectively; $p < 0.05$) islet cells treated with cytoEVs, which was fully reversed upon AMG487 addition (Figures 6D and S5). These results indicate immunogenicity of cytoEVs particularly on pancreatic islets, which is potentially mediated through cytoEV activation of the CXLCL10/CXCR3 pathway in islets.

DISCUSSION

Accumulating evidence suggests that EVs contribute to regulation of glucose homeostasis in health and under pathophysiological conditions in diabetes. Specifically, β cell-derived EVs appear to play a previously underappreciated role in modulating physiological responses to β cell pro-inflammatory stress (Guay et al., 2015; Palmisano et al., 2012; Sheng et al., 2011). In this study, we adopted a comprehensive approach by first performing detailed EV and proteomics cargo characterization of pro-inflammatory β cell-derived small EVs and then examined their biological role in modulating β cell insulin secretory function, transcriptome, and capacity for islet immune cell recruitment. We provide evidence of an inflammatory feedback loop in which diabetogenic pro-inflammatory cytokines induce CXCL10 production and packaging into small β cell EVs that, when secreted, target recipient β cells via direct binding to its receptor CXCR3 at the β cell surface. Activation of the CXCL10/CXCR3 axis induces the downstream pathways NF-κB and STAT1, which further exacerbate chemokine (*i.e.* CXCL10) production and packaging into small EVs, perpetuating the cycle of EV-mediated inflammation and β cell dysfunction. Moreover, promotion of a pro-inflammatory environment is perpetuated by the immunomodulatory role of cytoEVs through their ability to enhance antigen presentation and recruitment of cytotoxic $CD8^+$ T lymphocytes and macrophages.

Multiple deleterious biological effects of pro-inflammatory cytokines (e.g., IFNγ, TNF-α, and IL-1β) on β-cells have been well documented. In T1D, infiltrating T cells, macrophages, dendritic cells, and natural killer cells (Eizirik et al., 2009) are a primary source of cytokine production and secretion, where secreted diabetogenic cytokines have been shown to activate diverse pro-inflammatory intracellular signaling cascades (e.g., NF-κB, STAT1, etc.), resulting in the loss of β cell secretory function, β cell dedifferentiation, and eventual apoptosis-mediated cell death (Donath et al., 2003). Similarly, the chronic low-grade systemic inflammation observed in T2D activates similar signaling cascades, including

NF-κB, signaling, which has been a pharmacological target in clinical studies using salsalate (Fleischman et al., 2008; Goldfine et al., 2008; Salastekar et al., 2017) and the IL-1 receptor antagonist anakinra (Larsen et al., 2007). In this study, we provide evidence suggesting that pro-inflammatory cytokines also promote β cell functional failure through stimulation of β cell small EV secretion, which likely acts in a paracrine/autocrine manner to induce β cell dysfunction and enhance immune cell recruitment. The contribution of specific cytokines in the pathogenesis of T1D and T2D is debated in the literature. In the current study, cytokine combinations and concentrations were chosen based on previous reports of elevated IFNγ, TNF-α, and IL-1β in T1D (Cardozo et al., 2003; Nunemaker, 2016). However, it is important to note that other cytokines may play a critical role in induction of β cell dysfunction in T1D (Lu et al., 2020). Moreover, the individual effects of each cytokine on content and functional alterations of β cell-derived EVs have not been assessed but will be a topic for future studies.

In this study, our results show significant enrichment of the chemokine CXCL10 localized to the surface of these β cell-derived small EVs. Correspondingly, CXCL10-enriched EVs bind to CXCR3 surface receptors on β cells, leading to activation of pro-inflammatory pathways downstream of CXCR3 receptor activation (e.g., NF-κB and JAK/STAT1). Although the exact mechanistic link to β cell functional failure following cytoEV CXCL10/CXCR3 axis activation remains to be deciphered, a few potential mechanisms are plausible. Induction of STAT1 and NF-κB signaling has been shown to induce ER stress in β cells through inhibition of the ER Ca^{2+} pump SERCA2b and subsequent depletion of ER Ca^{2+} stores through induction of NF-κB-mediated nitric oxide (NO) production (Cardozo et al., 2005). However, reports have shown that this may be a species-dependent molecular event (Brozzi et al., 2015; Chan et al., 2012). Moreover, cytokine-mediated activation of STAT1 and NF-κB signaling in primary β cells was also found to downregulate several genes involved in β cell function (e.g., *Insulin*, *Glut2*, etc.) and identity (e.g., *Pdx1*, *MafA*, etc.) and stimulate chemokine production (e.g., *Cxcl10*) (Allagnat et al., 2010; Moore et al., 2011). Interestingly, blockade of the CXCR3 receptor with the compound AMG487 upon cytoEV addition restored expression of several of these β cell identity genes, suggesting a mechanistic link between the CXCR3 pathway and β cell functional failure. However, of note are the elevated expression levels of *Ins1* upon CXCR3 receptor blockade in the presence of cytoEVs. In the β cell, G protein-coupled receptors (GPCRs) typically stimulate insulin secretion through Gsα activation of the cyclic AMP (cAMP)/protein kinase A (PKA) pathway specifically by PKA activation to promote insulin transcription (Yang and Yang, 2016). On the other hand, β cells also express GPCRs that activate inhibitory G alpha proteins ($G\alpha_i$), suppressing insulin transcription (Metzemaekers et al., 2018), including CXCR3. Therefore, pharmacological inhibition of the CXCR3 receptor with AMG487 may restore cAMP levels, enhancing *Ins1* gene transcription. However, AMG487 may produce off-target effects that may enhance expression of *Ins1* transcription, as seen in Figure 5F. Future experiments will look into uncovering the mechanism of AMG487 action on insulin secretion to determine the optimal concentration for potential future *in vitro* and *in vivo* studies.

Intracellular β cell auto-antibodies to GAD65, IA-2, ZnT8, Glut2, and/or insulin in plasma or serum of individuals with T1D are present several years prior to clinical diagnosis and

have become predictive biomarkers for T1D onset (Winter and Schatz, 2011). Interestingly, many of these β cell auto-antigens have also been identified in β cell-derived EVs from rodent cell lines and islet-derived EVs from rat and human islets (Cianciaruso et al., 2017; Hasilo et al., 2017; Tesovnik et al., 2020). Moreover, recent evidence showed a distinct plasma EV-derived miRNA signature in EVs from individuals with T1D compared with healthy ctlEVs, suggesting the potential utility of EVs as clinical prognostic markers for T1D (Garcia-Contreras et al., 2017). Several reports have noted serum elevation of CXCL10 in T1D mouse models (Bender et al., 2017; Burke et al., 2016) and humans with T1D (Antonelli et al., 2014; Nicoletti et al., 2002; Shimada et al., 2001; Uno et al., 2010), with some studies reporting increased production of CXCL10 in pancreatic islets during the early stages of diabetes progression in mice (Cardozo et al., 2003; Li et al., 2005), in individuals newly diagnosed with T1D (Schulthess et al., 2009), and in those at high risk for the disease (Nicoletti et al., 2002). Additionally, a recent report implicated specific miRNAs in lymphocyte-derived EVs in inducing apoptosis and *Cxcl10* gene expression in β cells (Guay et al., 2019). These data, along with the work depicted here, suggest potential relevance of CXCL10 in diabetes, now with novel evidence of packaging and delivery to recipient β cells via small EVs to facilitate β cell inflammation, dysfunction, and immune cell recruitment. It is currently unclear when CXCL10 becomes enriched in EVs during T1D progression, but our work suggests that β cell EVs may facilitate this process early because of our lack of reported effects of these EVs on β cell apoptosis.

Destruction of pancreatic β cells by immune cell infiltrates is a key feature precipitating T1D pathogenesis. Analysis of human pancreatic sections from individuals with T1D revealed a key role of $CD4^+$ and $CD8^+$ T cells during β cell destruction (Pathiraja et al., 2015; Rodriguez-Calvo et al., 2014). This is believed to be achieved by the β cells' own complicit demise through events leading to aberrant processing/presentation of cellular antigens, rendering β cells susceptible to autoreactive T cell attack (Coppieters et al., 2012; Richardson et al., 2016). Both processes are accomplished by several means, including upregulated expression of MHC class I for $CD8^+$ T cells and class II for $CD4^+$ T cells (human leukocyte antigen [HLA] in humans) (Burrack et al., 2017). Here we show that pro-inflammatory β cell small EVs are capable of inducing gene transcripts associated with antigen processing/presentation in exposed islets and MHC class I and II protein expression in β and α cells. Moreover, antecedent exposure of these EVs to islets significantly enhanced cytotoxic $CD8^+$ lymphocyte and macrophage recruitment, which was reduced upon blockade of the CXCR3 receptor. However, the exact molecular mechanisms of pro-inflammatory β cell small EV induction of antigen processing and MHC class I and II presentation in β cells remains to be fully deduced. Evidence suggests that constitutive MHC class I expression is mediated by binding of NF-κB to promoter regions induced by cytokine activation (e.g., TNF-α) (Shirayoshi et al., 1987). Moreover, augmented expression of HLA-I (MHC) has been found in human T1 diabetic islets and correlated strongly with β cell STAT1 expression (Richardson et al., 2016), suggesting the potential mechanistic relevance of these transcription factors in pro-inflammatory β cell small EV induction of MHC class I expression in β cells.

Some reports have indicated conflicting evidence regarding the contribution of the CXCL10/CXCR3 axis in preclinical mouse models of T1D. *Cxcr3* knockout (KO) (Frigerio et al.,

2002) and CXCL10 antibody neutralization (Christen et al., 2003) substantially delayed onset of T1D; however, use of a small-molecule CXCR3 antagonist modestly delayed T1D but did not prevent onset in the RIP-LCMV-GP model (Christen et al., 2011). Moreover, *Cxcr3* deletion in NOD mice did not have an effect on T1D progression, but rather accelerated onset (Yamada et al., 2012). Because of the highly redundant nature of chemokine pathways, it is likely that several of these pathways work in congruence. Although we found only two chemokines to be highly enriched in β cell cytoEVs (CXCL9 and CXCL10), it may be plausible that other cargoes in cytoEVs play an independent or synergistic role in mediating β cell dysfunction and immune cell recruitment. Future studies will focus on further dissecting the role of other cytoEV components and their potential synergistic effects with CXCR3 pathway activation in mediating β cell failure under diabetogenic conditions.

In this work, we focused primarily on characterizing the small EV subtype from β cells under diabetogenic pro-inflammatory conditions. Previous work has implicated an association between packaging of β cell auto-antigens into small EVs (i.e., exosomes), particularly because of an association between exosome biogenesis via the endosomal pathway and the *trans*-Golgi secretory pathway, where several β cell auto-antigens are localized (Cianciaruso et al., 2017). Contrary to some reports (Guay et al., 2015; Lakhter et al., 2018), our findings, in addition to those of others (Cianciaruso et al., 2017; Giri et al., 2020), revealed that pro-inflammatory cytokines significantly enhanced small EV secretion from β cells. Thus, our focus and much of the focus in the β cell EV field has been primarily on the role of small EVs (mainly exosomes), with minimal insight into other subtypes of EVs (i.e., medium/large EVs or microvesicles and apoptotic bodies). As cells/tissues release vesicles of mixed populations with varying content and differing functional capabilities, there have been ongoing efforts in the EV field in recent years to assess EV heterogeneity. In the context of the β cell, understanding the contributions of each subtype of EVs and whether each population works independently or synergistically during diabetes pathogenesis will be critical to decipher. Recent work has found that pro-inflammatory cytokine exposure increased concentrations of small EV and apoptotic body subtypes in addition to increased cargo, including β cell auto-antigen, insulin, and immunostimulatory miRNA (Giri et al., 2020). Moreover, different subtypes of cytokine-exposed β cell EVs conferred varying degrees of immunogenicity when cultured *in vitro* with dendritic cells or macrophages (Giri et al., 2020).

Lastly, we noted that exposure of islets to cytoEVs caused β cell dysfunction but did not induce apoptosis. This finding contrasts with a recent report that indicated that cytokine-exposed MIN6 β cell EVs indeed stimulate β cell apoptosis in recipient cells (Guay et al., 2015). The differing results could be due to multiple factors, including a higher cytokine dosage used in the study by Guay et al. (2015), which may yield EVs with different cargo and/or concentrations of certain toxic cargoes capable of inducing higher rates of apoptosis. Moreover, we opted to use particle concentration (obtained by NTA) for our EV dosage strategy, with addition of EVs every day (2×10^9 particles/10 islets) for 48 h as opposed to a single addition of EVs using protein concentrations (50 μg/mL) incubated for 72 h (Guay et al., 2015). It is therefore plausible that these fundamental differences may affect the overall physiology of the islet/β cell in differing ways. Future studies should be conducted to

understand how cytokine dosage/timing affect EV cargo and function and how differing EV dosage strategies can affect overall β cell physiology.

Our study provides evidence of alterations in the intricate communication between β cells under diabetogenic stress mediated by production and release of CXCL10-bound pro-inflammatory small β cell EVs. Islet exposure to these EVs induced an inflammatory transcriptional landscape and promoted β cell dysfunction and antigen presentation. Mechanistically, we found that CXCL10-bound β cell EVs bound directly to β cell CXCR3 receptors and induced NFκB and STAT1 activation, which was reversed upon CXCR3 receptor antagonism. Moreover, blockade of the CXCL10/CXCR3 axis upon pro-inflammatory small β cell EV addition reduced overall MHC class I expression in β cells and $CD8^+$ T cell and macrophage recruitment to islets. Future work will involve further exploration of linking β cell functional alterations with the potential immunomodulatory role of CXCL10 EVs in development of diabetes with the goal of treatment and preventative strategies to restore functional β cell mass.

STAR★METHODS

RESOURCE AVAILABILITY

Lead contact—Further information and resource requests should be directed to and will be fulfilled by the lead contact, Naureen Javeed (javeed.naureen@mayo.edu).

Materials availability—This study did not generate new unique reagents.

Data and code availability—RNA-seq data have been deposited at NCBI GEO and proteomics data have been deposited to the ProteomeXchange Consortium via the PRIDE (Deutsch et al., 2020) partner repository. Accession numbers are listed in the key resources table and are publicly available as of the date of publication. This paper does not report original code. Any additional information required to reanalyze the data reported in this paper is available from the lead contact upon request.

EXPERIMENTAL MODEL AND SUBJECT DETAILS

Animal models—C57BL/6L male mice (Jackson Labs) were used for all *ex vivo* islet studies. Female NOD/ShlLtJ and control CD-1 IGS mice (Charles River Laboratories, Wilmington, MA) were obtained at 4 weeks. To generate multiple low-dose streptozotocin (MLD-STZ) mice, C57BL/6L mice were subjected to intraperitoneal injections of STZ (40 mg/kg/day in citrate buffer, pH 4.0) or vehicle (citrate buffer only) for five consecutive days (Sandberg et al., 1994). All mice were housed at Mayo Clinic Animal Facility under standard 12 h light, 12 h dark (LD) cycle, fed standard chow diet and experimental procedures were approved by Mayo Clinic Institutional Animal Care and Use Committee (IACUC).

Cell sources and materials—MIN6 cells were purchased from AddexBio, however the sex was not reported in the establishment of this cell line (Miyazaki et al., 1990). We have authenticated that this cell line expresses pancreatic β-cell identity genes including *Ins1/2*, *Pdx1*, and *MafA* by qRT-PCR. MIN6 cells were cultured in DMEM high glucose

media supplemented with 15% fetal bovine serum, 1 mM sodium pyruvate, and 50 μM β-mercaptoethanol. All mouse pro-inflammatory cytokines (IL-1β, TNFα, IFNγ) were purchased from R&D Systems (see Key resources table).

METHOD DETAILS

Isolation of small EVs—The protocol for isolation of EVs from cell culture medium was adapted from a previous study (Javeed et al., 2015). In brief, conditioned media was isolated and subjected to differential ultracentrifugation which includes 2 sequential spins at 2,000 x *g* for 30 min each, 1 spin at 10,000 x *g* for 30 min, filtration of the supernatant with a 0.2 μm filter, then 2 sequential spins at 100,000 x *g*, for 2 h each. The resulting pellets were resuspended in 1X PBS and stored with minimal freeze-thaw cycles at −80°C.

Nanoparticle Tracking Analysis of EVs—EV pellets were subjected to Nanoparticle Tracking Analysis (NTA; Malvern Panalytical) using the same dilution and NTA parameters for each fraction. For all runs, 4-5, 60 s videos were taken for each sample with representative NTA graphs shown for each condition.

EV internalization assay—MIN6 ctlEV were dyed with the ExoGlow-membrane EV labeling kit following manufacturer's protocol. In order to ensure the efficient removal of free dye, the resulting dyed ctlEV were re-precipitated using ExoQuick-TC solution and resuspended in 1X PBS. 10 μl of labeled ctlEV were added to freshly isolated C57BL/6L mouse islets (Rakshit et al., 2016) and images were acquired at 40X after 1h incubation using a Zeiss LSM 780 confocal microscope.

Transmission electron microscopy imaging of β-cell EVs—Isolated MIN6 EVs were allowed to adhere to formvar coated 200 mesh copper grids (EMS, Hatfield, PA), rinsed with dH_2O and stained with 1% aqueous phosphotungstic acid, pH 7.0 (EMS). Transmission electron microscopy was performed using a JEOL 1400+ operating at 80kV.

Immunofluorescence staining and quantification—Isolated mouse pancreas or islets were fixed in 4% paraformaldehyde overnight and paraffin embedded. Deparaffinized sections were co-immunostained to assess β-cell apoptosis using terminal deoxynucleotidyl transferase dUTP nick end labeling (TUNEL) and insulin (1:100). Adjacent sections were co-immunostained for Ki67 (1:40) and insulin (1:100) to assess β-cell proliferation. Additional sections were used to stain for phospho-proteins p-p65 (1:1000) and p-STAT1 (1:500), HLA-ABC (1:100), and MHC class II (1:200) along with insulin (noted above) and glucagon (1:1000). CXCL10 (1μg/ml) along with insulin and glucagon noted above were used to stain paraffin embedded islets and pancreas sections from NOD, MLD-STZ and C57BL/6L mice. DAPI mounting medium was used for all slides and each were imaged and analyzed using a Zeiss Axio Observer Z1 microscope (Carl Zeiss Microscopy, LLC) and ZenPro software (Carl Zeiss Microscopy, LLC). Quantification of Ki67 and TUNEL staining was analyzed using ImageJ cell counter and expressed as percent positive per β-cell or α-cell. Quantification of insulin area, HLA-ABC (MHC class I), and MHC class II staining was analyzed using ImageJ color threshold and expressed as a percent average insulin positive area per islet.

Mouse islet isolation and glucose stimulated insulin secretion assay—Mouse islets were isolated from C57BL/6L mice (Jackson Labs) using a standard collagenase method as previously described (Rakshit et al., 2016). Islets were recovered overnight in standard RPMI 1640 media supplemented with 10% fetal bovine serum and penicillin/streptomycin solution. 10 mouse islets/well were treated with GW4869 (5 μM) and/or cytomix combination (IL-1β (0.2 ng/ml), TNFα (10 ng/ml), IFNγ (10 ng/ml)), for 24 h. For cytoEV studies, 10 islets/well were treated with $2X10^9$ particles every day for 48 h. To measure static glucose stimulated insulin secretion (GSIS) 10 islets/well were incubated first in Krebs Ringer buffer (KRB) supplemented with 4 mM glucose for 30 minutes followed by exposure to KRB buffer containing 16 mM glucose for 30 minutes. Insulin was measured by using an ultrasensitive mouse insulin ELISA kit. Insulin values were normalized by either total islet number or insulin content.

Quantitative real-time polymerase chain reaction (qRT-PCR) analysis—Total RNA was extracted with the RNeasy Mini kit and complement DNA (cDNA) was transcribed from 100 ng of RNA using the iScript cDNA Synthesis kit. SYBR Green Master mix was added to the cDNA with the gene-specific primers. Mouse primers used are listed in Table S1. Gene expression analysis was performed using the ABI StepOnePlus Real-Time PCR System and analyzed using ΔΔCT method normalized to *Gapdh*.

Western blot analysis—MIN6 cells were lysed in NP40 lysis buffer supplemented with protease cocktail inhibitor (1:100) following various treatments. For blotting of EV fractions, sonication was done 3X, 30 s each. Lysates were centrifuged at 14,000 rpm for 10 mins at 4°C to remove cell debris. Protein concentrations were assessed using a bicinchoninic acid (BCA) protein assay. Equal amounts of protein lysates were denatured at 95°C for 5 min in SDS sample buffer and subjected to SDS-PAGE (TGX 4%–20% gradient gels) and immunoblotting. The blots were blocked in 5% non-fat milk powder made with 1X tris buffer saline solution (TBS). Overnight incubation at 4°C occurred using the following primary antibodies: CD9, ALIX, TSG101, CXCL10, RAB7, GAPDH, β-actin. Corresponding secondary antibodies were used and images and quantification of bands were done using the Li-Cor Odyssey Fc with Image Studio (Version 4.0) software. Source identification and dilutions are listed in the Key resources table.

RNA-Seq analysis—mRNA was isolated using a RNeasy Plus Minikit. RNA quality was determined using the Fragment Analyzer from Agilent. RNA libraries were prepared using 200 ng of total RNA according to the manufacturer's instructions for the TruSeq Stranded mRNA Sample Prep Kit (Illumina, San Diego, CA). Fragment reads were aligned using TopHat version 2.0.6 (Trapnell et al., 2012), assembled using StringTie version 2.1.3 (Pertea et al., 2015), and counted using StringTie's script (PrepDE.py) via Python version 3.6, all with default settings. The count matrix was then imported into R version 3.6.1 and differentially expressed genes were identified using edgeR version 3.1.1 (Robinson et al., 2010) using a cutoff of $p < 0.05$ and a fold change greater than 1.5. These differentially expressed genes were then submitted for ontological analysis using the WEB-based Gene Set Analysis Toolkit (WebGestalt) (Liao et al., 2019) against Kyoto Encyclopedia of Genes and Genomes (KEGG) curated pathways. Significantly enriched

KEGG pathways ($p < 0.05$) were visualized using Cytoscape version 3.7.1 (Shannon et al., 2003). Protein-protein interactions of significantly enriched transcripts were assessed using the STRING Protein-Protein Interaction Network version 11 (Szklarczyk et al., 2015). Gene-set enrichment analysis (GSEA) was conducted via GSEA 4.0.1 of curated pathways from the Molecular Signatures Database using default settings and considered significantly enriched at $p < 0.05$ (Subramanian et al., 2005). *De novo* motif enrichment was subsequently performed on promoter regions of differentially expressed transcripts using HOMER v4.10 using the findMotifs.pl function with default settings. Significantly enriched motifs were identified with p < 1e-12 (false positive threshold). Best matching motifs were identified, provided their match scores exceeded 0.80 (Ramos-Rodríguez et al., 2019). If best matching motifs did not reach this threshold, the top 3 matches associated with the enriched motif were identified. Rank-Rank Hypergeometric Overlap (RRHO) analysis was conducted by first converting mouse genes to human orthologs using Biomart. RRHO was performed on ranked fold changes of T1D versus non-diabetic (ND) and cytoEV treatment versus untreated islets using default settings (Plaisier et al., 2010).

Proteomics analysis of β-cell EV content—Pelleted EVs were resuspended in 50 ul of 2% SDS and protein content was determined using a BCA assay. Proteolytic digestion took place with the addition of trypsin at a ratio of 1:50 (wt:wt) followed by a 16h overnight incubation. A normalized amount of the resulting peptides were analyzed by nano liquid chromatography–tandem mass spectrometry (nLC-MS/MS). Eluting peptides were analyzed using an Orbitrap Fusion Lumos (Thermo Scientific) mass spectrometer operated in data dependent mode. Raw files were processed in MaxQuant software version 1.6.0.1. Spectra were searched using the Andromeda search engine against the mouse SwissProt database downloaded May 9th, 2018. N-terminal acetylation and methionine oxidation were set as variable modifications and cysteine carbamidomethylation was set to fixed modification. Searches were performed with a false discovery rate of 1% for both peptides and proteins using a target-decoy approach. A two peptide minimum was required, peptide length was at least 7 amino acids long and MS2 match tolerance was set to 0.02Da. Match between runs was enabled with a retention time window of 0.7min. Enzyme specificity was set to trypsin and a maximum of 2 missed cleavages were allowed. Protein data was extracted from the “proteinGroups.txt” file and all mass spectrometry data was processed using custom R scripts. Significantly up and downregulated proteins were determined by using Log_2(fold change) > 1 and then subjected to pathway analysis using Panther Go Slim.

Proteinase K treatment of EVs—The protocol for digestion of membrane bound proteins on cytoEV was adapted from previous literature (Cvjetkovic et al., 2016). In brief, 20 μg/ml of proteinase K (diluted in Tris-HCl) with 5 mM $CaCl^2$ was added to cytoEV and incubated at 37°C for 1 h. Protease activity was inhibited with the addition of 5 mM phenylmethylsulfonyl fluoride for 10 minutes at room temperature. To assess digested surface proteins the sample along with an equal amount of undigested cytoEV sample from the same isolation batch were prepared for western blotting analysis as indicated above.

***In situ* proximity ligation assay—**Proximity ligation assay (PLA) protocol was adapted from previous work (Javeed et al., 2015; Pearson and Soleimanpour, 2019). In brief, isolated

C57BL/6L mouse islets were cultured with the appropriate conditions (αCXCL10 (25 μg/ml), cytomix, (IL-1β (0.2 ng/ml), TNFα (10 ng/ml), IFNγ (10 ng/ml)), cytoEV ($8X10^9$/day), AMG487 (1 μM), MedChemExpress; ~50 islets per condition). After 48 h, islets were washed in cold 1X PBS and dissociated with 1X Cell Dissociation Buffer. Dispersed islets were treated with 4% paraformaldehyde for 10 mins, blocked with 10% donkey serum for 1 h, then incubated with primary antibodies for CXCL10 (10 μg/ml), CXCR3 (1:100), and insulin (1:100) overnight at 4°C. PLA probe incubation, ligation, and amplification steps were followed as per manufacturer's protocol with the addition of secondary anti-guinea pig Cy5 antibody (1:100) added to the probe solution to detect insulin expression (Pearson and Soleimanpour, 2019). Images were taken at 20X using a Zeiss Axio Observer Z1 microscope for PLA dot quantification and single β-cell high resolution images were taken on a Zeiss LSM 780 confocal microscope at 40X. Quantification of β-cell positive PLA dots was conducted using ImageJ software using consistent threshold values for each image.

Isolation of bone marrow-derived macrophages, $CD8^+$ T cells, and chemotaxis assay—Isolation of bone marrow-derived macrophages (BMDMs) was completed as previously described (Zhang et al., 2008). In brief, C57BL/6L mice were euthanized and BMDMs were extracted from both femurs and tibias. Bone marrow progenitor cells were cultured in macrophage complete medium (basal endothelial media supplemented with 10% FBS, penicillin-streptomycin, and GM-CSF). After day 7, BMDMs were harvested and $1X10^6$ cells were counted and assessed for purity using flow cytometry analysis of BMDM markers F4/80 and CD11b (> 98%, data not shown). The remaining BMDMs were cultured in DMEM/F12 media supplemented with 10% FBS. For isolation of $CD8^+$ T cells, spleen was isolated from C57BL/6L mice and T cells were isolated using the EasySep Mouse $CD8^+$ T Cell isolation kit as per manufacturer protocol. The purity of the $CD8^+$ T cell population was determined to be > 95% as assessed by flow cytometry (data not shown). For the chemotaxis assay, the CytoSelect Chemotaxis Assay kit (5 μm, 24 well format) was used per manufacturer protocol. In brief, 10 C57BL/6L mouse islets/treatment group were cultured in EV-free media for 24 h prior to the assay. Islets were then transferred along with 500 μl of the original media to a 24 well plate. $1X10^6$ $CD8^+$ T cells or BMDMs/condition were added to the top insert at a final volume of 100 μl. After 8 h the cells were dissociated from the bottom of the insert and added to the migrated cells then dyed with CyQuant GR dye solution. Fluorescence was read using a Biotek Synergy H3 plate reader at 480 nm/520 nm.

QUANTIFICATION AND STATISTICAL ANALYSIS

Statistical analysis was performed using standard Student's t tests with Mann-Whitney post hoc tests (for comparison of 2 groups) or one-way ANOVA with Kruskal-Wallis post hoc tests (for multiple group comparisons; GraphPad Prizm v.6.0). The data was presented as a mean ± SEM with significance noted as $p < 0.05$. Sample size for each experiment are displayed in the figure legends.

Supplementary Material

Refer to Web version on PubMed Central for supplementary material.

ACKNOWLEDGMENTS

We acknowledge funding support from the National Institutes of Health (R01DK098468 to A.V.M., T32-HL105355 to N.J., and F99DK123834 to M.R.B.), the James A. Ruppe Career Development Award in Endocrinology (Mayo Clinic, Rochester, MN, to N.J.), the CCaTS-CBD Pilot Award for Team Science (Mayo Clinic, Rochester, MN, to A.V.M., A.V., and N.J.), and the Center for Regenerative Medicine (Mayo Clinic, Rochester, MN).

REFERENCES

Allagnat F, Christulia F, Ortis F, Pirot P, Lortz S, Lenzen S, Eizirik DL, and Cardozo AK (2010). Sustained production of spliced X-box binding protein 1 (XBP1) induces pancreatic beta cell dysfunction and apoptosis. Diabetologia 53, 1120–1130. [PubMed: 20349222]

Antonelli A, Ferrari SM, Corrado A, Ferrannini E, and Fallahi P (2014). CXCR3, CXCL10 and type 1 diabetes. Cytokine Growth Factor Rev. 25, 57–65. [PubMed: 24529741]

Bashratyan R, Sheng H, Regn D, Rahman MJ, and Dai YD (2013). Insulinoma-released exosomes activate autoreactive marginal zone-like B cells that expand endogenously in prediabetic NOD mice. Eur. J. Immunol 43, 2588–2597. [PubMed: 23817982]

Bender C, Christen S, Scholich K, Bayer M, Pfeilschifter JM, Hintermann E, and Christen U (2017). Islet-Expressed CXCL10 Promotes Autoimmune Destruction of Islet Isografts in Mice With Type 1 Diabetes. Diabetes 66, 113–126. [PubMed: 27797910]

Brozzi F, Nardelli TR, Lopes M, Millard I, Barthson J, Igoillo-Esteve M, Grieco FA, Villate O, Oliveira JM, Casimir M, et al. (2015). Cytokines induce endoplasmic reticulum stress in human, rat and mouse beta cells via different mechanisms. Diabetologia 58, 2307–2316. [PubMed: 26099855]

Burke SJ, Stadler K, Lu D, Gleason E, Han A, Donohoe DR, Rogers RC, Hermann GE, Karlstad MD, and Collier JJ (2015). IL-1β reciprocally regulates chemokine and insulin secretion in pancreatic β-cells via NF-κB. Am. J. Physiol. Endocrinol. Metab 309, E715–E726. [PubMed: 26306596]

Burke SJ, Karlstad MD, Eder AE, Regal KM, Lu D, Burk DH, and Collier JJ (2016). Pancreatic β-Cell production of CXCR3 ligands precedes diabetes onset. Biofactors 42, 703–715. [PubMed: 27325565]

Burrack AL, Martinov T, and Fife BT (2017). T Cell-Mediated Beta Cell Destruction: Autoimmunity and Alloimmunity in the Context of Type 1 Diabetes. Front. Endocrinol. (Lausanne) 8, 343. [PubMed: 29259578]

Butler AE, Janson J, Bonner-Weir S, Ritzel R, Rizza RA, and Butler PC (2003). Beta-cell deficit and increased beta-cell apoptosis in humans with type 2 diabetes. Diabetes 52, 102–110. [PubMed: 12502499]

Cardozo AK, Proost P, Gysemans C, Chen MC, Mathieu C, and Eizirik DL (2003). IL-1beta and IFN-gamma induce the expression of diverse chemokines and IL-15 in human and rat pancreatic islet cells, and in islets from prediabetic NOD mice. Diabetologia 46, 255–266. [PubMed: 12627325]

Cardozo AK, Ortis F, Storling J, Feng YM, Rasschaert J, Tonnesen M, Van Eylen F, Mandrup-Poulsen T, Herchuelz A, and Eizirik DL (2005). Cytokines downregulate the sarcoendoplasmic reticulum pump Ca2+ ATPase 2b and deplete endoplasmic reticulum Ca2+, leading to induction of endoplasmic reticulum stress in pancreatic beta-cells. Diabetes 54, 452–461. [PubMed: 15677503]

Chan JY, Biden TJ, and Laybutt DR (2012). Cross-talk between the unfolded protein response and nuclear factor-κB signalling pathways regulates cytokine-mediated beta cell death in MIN6 cells and isolated mouse islets. Diabetologia 55, 2999–3009. [PubMed: 22893028]

Christen U, McGavern DB, Luster AD, von Herrath MG, and Oldstone MB (2003). Among CXCR3 chemokines, IFN-gamma-inducible protein of 10 kDa (CXC chemokine ligand (CXCL) 10) but not monokine induced by IFN-gamma (CXCL9) imprints a pattern for the subsequent development of autoimmune disease. J. Immunol 171, 6838–6845. [PubMed: 14662890]

Christen S, Holdener M, Beerli C, Thoma G, Bayer M, Pfeilschifter JM, Hintermann E, Zerwes HG, and Christen U (2011). Small molecule CXCR3 antagonist NIBR2130 has only a limited impact on type 1 diabetes in a virus-induced mouse model. Clin. Exp. Immunol 165, 318–328. [PubMed: 21649647]

Cianciaruso C, Phelps EA, Pasquier M, Hamelin R, Demurtas D, Alibashe Ahmed M, Piemonti L, Hirosue S, Swartz MA, De Palma M, et al. (2017). Primary Human and Rat β-Cells Release the

Intracellular Autoantigens GAD65, IA-2, and Proinsulin in Exosomes Together With Cytokine-Induced Enhancers of Immunity. Diabetes 66, 460–473. [PubMed: 27872147]

Coppieters KT, Dotta F, Amirian N, Campbell PD, Kay TW, Atkinson MA, Roep BO, and von Herrath MG (2012). Demonstration of islet-autoreactive CD8 T cells in insulitic lesions from recent onset and long-term type 1 diabetes patients. J. Exp. Med 209, 51–60. [PubMed: 22213807]

Cvjetkovic A, Jang SC, Konečná B, Höög JL, Sihlbom C, Lässer C, and Lötvall J (2016). Detailed Analysis of Protein Topology of Extracellular Vesicles-Evidence of Unconventional Membrane Protein Orientation. Sci. Rep 6, 36338. [PubMed: 27821849]

Deutsch EW, Bandeira N, Sharma V, Perez-Riverol Y, Carver JJ, Kundu DJ, García-Seisdedos D, Jarnuczak AF, Hewapathirana S, Pullman BS, et al. (2020). The ProteomeXchange consortium in 2020: enabling 'big data' approaches in proteomics. Nucleic Acids Res. 48 (D1), D1145–D1152. [PubMed: 31686107]

Devaiah BN, and Singer DS (2013). CIITA and Its Dual Roles in MHC Gene Transcription. Front. Immunol 4, 476. [PubMed: 24391648]

Donath MY, Størling J, Maedler K, and Mandrup-Poulsen T (2003). Inflammatory mediators and islet beta-cell failure: a link between type 1 and type 2 diabetes. J. Mol. Med. (Berl.) 81, 455–470. [PubMed: 12879149]

Eguchi A, Lazic M, Armando AM, Phillips SA, Katebian R, Maraka S, Quehenberger O, Sears DD, and Feldstein AE (2016). Circulating adipocyte-derived extracellular vesicles are novel markers of metabolic stress. J. Mol. Med. (Berl.) 94, 1241–1253. [PubMed: 27394413]

Eizirik DL, Colli ML, and Ortis F (2009). The role of inflammation in insulitis and beta-cell loss in type 1 diabetes. Nat. Rev. Endocrinol 5, 219–226. [PubMed: 19352320]

Essandoh K, Yang L, Wang X, Huang W, Qin D, Hao J, Wang Y, Zingarelli B, Peng T, and Fan GC (2015). Blockade of exosome generation with GW4869 dampens the sepsis-induced inflammation and cardiac dysfunction. Biochim. Biophys. Acta 1852, 2362–2371. [PubMed: 26300484]

Fleischman A, Shoelson SE, Bernier R, and Goldfine AB (2008). Salsalate improves glycemia and inflammatory parameters in obese young adults. Diabetes Care 31, 289–294. [PubMed: 17959861]

Freeman DW, Noren Hooten N, Eitan E, Green J, Mode NA, Bodogai M, Zhang Y, Lehrmann E, Zonderman AB, Biragyn A, et al. (2018). Altered Extracellular Vesicle Concentration, Cargo, and Function in Diabetes. Diabetes 67, 2377–2388. [PubMed: 29720498]

Frigerio S, Junt T, Lu B, Gerard C, Zumsteg U, Holländer GA, and Piali L (2002). Beta cells are responsible for CXCR3-mediated T-cell infiltration in insulitis. Nat. Med 8, 1414–1420. [PubMed: 12415259]

Garcia-Contreras M, Shah SH, Tamayo A, Robbins PD, Golberg RB, Mendez AJ, and Ricordi C (2017). Plasma-derived exosome characterization reveals a distinct microRNA signature in long duration Type 1 diabetes. Sci. Rep 7, 5998. [PubMed: 28729721]

Giri KR, de Beaurepaire L, Jegou D, Lavy M, Mosser M, Dupont A, Fleurisson R, Dubreil L, Collot M, Van Endert P, et al. (2020). Molecular and Functional Diversity of Distinct Subpopulations of the Stressed Insulin-Secreting Cell's Vesiculome. Front. Immunol 11, 1814. [PubMed: 33101266]

Goldfine AB, Silver R, Aldhahi W, Cai D, Tatro E, Lee J, and Shoelson SE (2008). Use of salsalate to target inflammation in the treatment of insulin resistance and type 2 diabetes. Clin. Transl. Sci 1, 36–43. [PubMed: 19337387]

Guay C, Menoud V, Rome S, and Regazzi R (2015). Horizontal transfer of exosomal microRNAs transduce apoptotic signals between pancreatic beta-cells. Cell Commun. Signal 13, 17. [PubMed: 25880779]

Guay C, Kruit JK, Rome S, Menoud V, Mulder NL, Jurdzinski A, Mancarella F, Sebastiani G, Donda A, Gonzalez BJ, et al. (2019). Lymphocyte-Derived Exosomal MicroRNAs Promote Pancreatic β Cell Death and May Contribute to Type 1 Diabetes Development. Cell Metab. 29, 348–361.e6. [PubMed: 30318337]

Hamilton-Williams EE, Palmer SE, Charlton B, and Slattery RM (2003). Beta cell MHC class I is a late requirement for diabetes. Proc. Natl. Acad. Sci. USA 100, 6688–6693. [PubMed: 12750472]

Hasilo CP, Negi S, Allaeys I, Cloutier N, Rutman AK, Gasparrini M, Bonneil Á, Thibault P, Boilard Á, and Paraskevas S (2017). Presence of diabetes autoantigens in extracellular vesicles derived from human islets. Sci. Rep 7, 5000. [PubMed: 28694505]

Javeed N (2019). Shedding Perspective on Extracellular Vesicle Biology in Diabetes and Associated Metabolic Syndromes. Endocrinology 160, 399–408. [PubMed: 30624638]

Javeed N, Sagar G, Dutta SK, Smyrk TC, Lau JS, Bhattacharya S, Truty M, Petersen GM, Kaufman RJ, Chari ST, and Mukhopadhyay D (2015). Pancreatic Cancer-Derived Exosomes Cause Paraneoplastic β-cell Dysfunction. Clin. Cancer Res. 21, 1722–1733. [PubMed: 25355928]

Kahn SE, Zraika S, Utzschneider KM, and Hull RL (2009). The beta cell lesion in type 2 diabetes: there has to be a primary functional abnormality. Diabetologia 52, 1003–1012. [PubMed: 19326096]

Kalluri R, and LeBleu VS (2020). The biology, function, and biomedical applications of exosomes. Science 367, eaau6977. [PubMed: 32029601]

Lakhter AJ, Pratt RE, Moore RE, Doucette KK, Maier BF, DiMeglio LA, and Sims EK (2018). Beta cell extracellular vesicle miR-21-5p cargo is increased in response to inflammatory cytokines and serves as a biomarker of type 1 diabetes. Diabetologia 61, 1124–1134. [PubMed: 29445851]

Larsen CM, Faulenbach M, Vaag A, Vølund A, Ehses JA, Seifert B, Mandrup-Poulsen T, and Donath MY (2007). Interleukin-1-receptor antagonist in type 2 diabetes mellitus. N. Engl. J. Med 356, 1517–1526. [PubMed: 17429083]

Li D, Zhu SW, Liu DJ, and Liu GL (2005). Expression of interferon inducible protein-10 in pancreas of mice. World J. Gastroenterol 11, 4750–4752. [PubMed: 16094723]

Liao Y, Wang J, Jaehnig EJ, Shi Z, and Zhang B (2019). WebGestalt 2019: gene set analysis toolkit with revamped UIs and APIs. Nucleic Acids Res. 47, W199–W205. [PubMed: 31114916]

Lu J, Liu J, Li L, Lan Y, and Liang Y (2020). Cytokines in type 1 diabetes: mechanisms of action and immunotherapeutic targets. Clin. Transl. Immunology 9, e1122. [PubMed: 32185024]

Mathivanan S, Ji H, and Simpson RJ (2010). Exosomes: extracellular organelles important in intercellular communication. J. Proteomics 73, 1907–1920. [PubMed: 20601276]

Matveyenko AV, and Butler PC (2008). Relationship between beta-cell mass and diabetes onset. Diabetes Obes. Metab 10 (Suppl 4), 23–31. [PubMed: 18834430]

Meier JJ, Bhushan A, Butler AE, Rizza RA, and Butler PC (2005). Sustained beta cell apoptosis in patients with long-standing type 1 diabetes: indirect evidence for islet regeneration? Diabetologia 48, 2221–2228. [PubMed: 16205882]

Metzemaekers M, Vanheule V, Janssens R, Struyf S, and Proost P (2018). Overview of the Mechanisms that May Contribute to the Non-Redundant Activities of Interferon-Inducible CXC Chemokine Receptor 3 Ligands. Front. Immunol 8, 1970. [PubMed: 29379506]

Miyazaki J, Araki K, Yamato E, Ikegami H, Asano T, Shibasaki Y, Oka Y, and Yamamura K (1990). Establishment of a pancreatic beta cell line that retains glucose-inducible insulin secretion: special reference to expression of glucose transporter isoforms. Endocrinology 127, 126–132. [PubMed: 2163307]

Moin ASM, and Butler AE (2019). Alterations in Beta Cell Identity in Type 1 and Type 2 Diabetes. Curr. Diab. Rep 19, 83. [PubMed: 31401713]

Moore F, Naamane N, Colli ML, Bouckenooghe T, Ortis F, Gurzov EN, Igoillo-Esteve M, Mathieu C, Bontempi G, Thykjaer T, et al. (2011). STAT1 is a master regulator of pancreatic beta-cell apoptosis and islet inflammation. J. Biol. Chem 286, 929–941. [PubMed: 20980260]

Nicoletti F, Conget I, Di Mauro M, Di Marco R, Mazzarino MC, Bendtzen K, Messina A, and Gomis R (2002). Serum concentrations of the interferon-gamma-inducible chemokine IP-10/CXCL10 are augmented in both newly diagnosed Type I diabetes mellitus patients and subjects at risk of developing the disease. Diabetologia 45, 1107–1110. [PubMed: 12189440]

Nunemaker CS (2016). Considerations for Defining Cytokine Dose, Duration, and Milieu That Are Appropriate for Modeling Chronic Low-Grade Inflammation in Type 2 Diabetes. J. Diabetes Res 2016, 2846570. [PubMed: 27843953]

Palmisano G, Jensen SS, Le Bihan MC, Lainé J, McGuire JN, Pociot F, and Larsen MR (2012). Characterization of membrane-shed microvesicles from cytokine-stimulated β-cells using proteomics strategies. Mol. Cell. Proteomics 11, 230–243. [PubMed: 22345510]

Pathiraja V, Kuehlich JP, Campbell PD, Krishnamurthy B, Loudovaris T, Coates PT, Brodnicki TC, O'Connell PJ, Kedzierska K, Rodda C, et al. (2015). Proinsulin-specific, HLA-DQ8, and HLA-

DQ8-transdimer-restricted CD4+ T cells infiltrate islets in type 1 diabetes. Diabetes 64, 172–182. [PubMed: 25157096]

Pearson G, and Soleimanpour SA (2019). Visualization of Endogenous Mitophagy Complexes In Situ in Human Pancreatic Beta Cells Utilizing Proximity Ligation Assay. J. Vis. Exp (147)

Pertea M, Pertea GM, Antonescu CM, Chang T-C, Mendell JT, and Salzberg SL (2015). StringTie enables improved reconstruction of a transcriptome from RNA-seq reads. Nat. Biotechnol 33, 290–295. [PubMed: 25690850]

Plaisier SB, Taschereau R, Wong JA, and Graeber TG (2010). Rank-rank hypergeometric overlap: identification of statistically significant overlap between gene-expression signatures. Nucleic Acids Res. 38, e169. [PubMed: 20660011]

Rakshit K, Qian J, Ernst J, and Matveyenko AV (2016). Circadian variation of the pancreatic islet transcriptome. Physiol. Genomics 48, 677–687. [PubMed: 27495157]

Ramos-Rodríguez M, Raurell-Vila H, Colli ML, Alvelos MI, Subirana-Granés M, Juan-Mateu J, Norris R, Turatsinze JV, Nakayasu ES, Webb-Robertson BM, et al. (2019). The impact of proinflammatory cytokines on the β-cell regulatory landscape provides insights into the genetics of type 1 diabetes. Nat. Genet 51, 1588–1595. [PubMed: 31676868]

Richardson SJ, Rodriguez-Calvo T, Gerling IC, Mathews CE, Kaddis JS, Russell MA, Zeissler M, Leete P, Krogvold L, Dahl-Jørgensen K, et al. (2016). Islet cell hyperexpression of HLA class I antigens: a defining feature in type 1 diabetes. Diabetologia 59, 2448–2458. [PubMed: 27506584]

Robinson MD, McCarthy DJ, and Smyth GK (2010). edgeR: a Bioconductor package for differential expression analysis of digital gene expression data. Bioinformatics 26, 139–140. [PubMed: 19910308]

Rodriguez-Calvo T, Ekwall O, Amirian N, Zapardiel-Gonzalo J, and von Herrath MG (2014). Increased immune cell infiltration of the exocrine pancreas: a possible contribution to the pathogenesis of type 1 diabetes. Diabetes 63, 3880–3890. [PubMed: 24947367]

Russell MA, Redick SD, Blodgett DM, Richardson SJ, Leete P, Krogvold L, Dahl-Jørgensen K, Bottino R, Brissova M, Spaeth JM, et al. (2019). HLA Class II Antigen Processing and Presentation Pathway Components Demonstrated by Transcriptome and Protein Analyses of Islet β-Cells From Donors With Type 1 Diabetes. Diabetes 68, 988–1001. [PubMed: 30833470]

Rutman AK, Negi S, Gasparrini M, Hasilo CP, Tchervenkov J, and Paraskevas S (2018). Immune Response to Extracellular Vesicles From Human Islets of Langerhans in Patients With Type 1 Diabetes. Endocrinology 159, 3834–3847. [PubMed: 30307543]

Salastekar N, Desai T, Hauser T, Schaefer EJ, Fowler K, Joseph S, Shoelson SE, and Goldfine AB; TINSAL-CVD study team (2017). Salsalate improves glycaemia in overweight persons with diabetes risk factors of stable statin-treated cardiovascular disease: A 30-month randomized placebo-controlled trial. Diabetes Obes. Metab 19, 1458–1462. [PubMed: 28295931]

Sandberg JO, Andersson A, Eizirik DL, and Sandler S (1994). Interleukin-1 receptor antagonist prevents low dose streptozotocin induced diabetes in mice. Biochem. Biophys. Res. Commun 202, 543–548. [PubMed: 8037760]

Schulthess FT, Paroni F, Sauter NS, Shu L, Ribaux P, Haataja L, Strieter RM, Oberholzer J, King CC, and Maedler K (2009). CXCL10 impairs beta cell function and viability in diabetes through TLR4 signaling. Cell Metab. 9, 125–139. [PubMed: 19187771]

Shannon P, Markiel A, Ozier O, Baliga NS, Wang JT, Ramage D, Amin N, Schwikowski B, and Ideker T (2003). Cytoscape: a software environment for integrated models of biomolecular interaction networks. Genome Res. 13, 2498–2504. [PubMed: 14597658]

Sheng H, Hassanali S, Nugent C, Wen L, Hamilton-Williams E, Dias P, and Dai YD (2011). Insulinoma-released exosomes or microparticles are immunostimulatory and can activate autoreactive T cells spontaneously developed in nonobese diabetic mice. J. Immunol 187, 1591–1600. [PubMed: 21734072]

Sherry NA, Tsai EB, and Herold KC (2005). Natural history of beta-cell function in type 1 diabetes. Diabetes 54 (Suppl 2), S32–S39. [PubMed: 16306337]

Shimada A, Morimoto J, Kodama K, Suzuki R, Oikawa Y, Funae O, Kasuga A, Saruta T, and Narumi S (2001). Elevated serum IP-10 levels observed in type 1 diabetes. Diabetes Care 24, 510–515. [PubMed: 11289477]

Shirayoshi Y, Miyazaki J, Burke PA, Hamada K, Appella E, and Ozato K (1987). Binding of multiple nuclear factors to the 5′ upstream regulatory element of the murine major histocompatibility class I gene. Mol. Cell. Biol 7, 4542–4548. [PubMed: 3501825]

Sims EK, Mirmira RG, and Evans-Molina C (2020). The role of beta-cell dysfunction in early type 1 diabetes. Curr. Opin. Endocrinol. Diabetes Obes 27, 215–224. [PubMed: 32618633]

Subramanian A, Tamayo P, Mootha VK, Mukherjee S, Ebert BL, Gillette MA, Paulovich A, Pomeroy SL, Golub TR, Lander ES, and Mesirov JP (2005). Gene set enrichment analysis: a knowledge-based approach for interpreting genome-wide expression profiles. Proc. Natl. Acad. Sci. USA 102, 15545–15550. [PubMed: 16199517]

Szklarczyk D, Franceschini A, Wyder S, Forslund K, Heller D, Huerta-Cepas J, Simonovic M, Roth A, Santos A, Tsafou KP, et al. (2015). STRING v10: protein-protein interaction networks, integrated over the tree of life. Nucleic Acids Res. 43, D447–D452. [PubMed: 25352553]

Tesovnik T, Kovač J, Pohar K, Hudoklin S, Dovč K, Bratina N, Trebušak Podkrajšek K, Debeljak M, Veranič P, Bosi E, et al. (2020). Extracellular Vesicles Derived Human-miRNAs Modulate the Immune System in Type 1 Diabetes. Front. Cell Dev. Biol 8, 202. [PubMed: 32296701]

Théry C, Witwer KW, Aikawa E, Alcaraz MJ, Anderson JD, Andriantsitohaina R, Antoniou A, Arab T, Archer F, Atkin-Smith GK, et al. (2018). Minimal information for studies of extracellular vesicles 2018 (MISEV2018): a position statement of the International Society for Extracellular Vesicles and update of the MISEV2014 guidelines. J. Extracell. Vesicles 7, 1535750. [PubMed: 30637094]

Trapnell C, Roberts A, Goff L, Pertea G, Kim D, Kelley DR, Pimentel H, Salzberg SL, Rinn JL, and Pachter L (2012). Differential gene and transcript expression analysis of RNA-seq experiments with TopHat and Cufflinks. Nat. Protoc 7, 562–578. [PubMed: 22383036]

Uno S, Imagawa A, Saisho K, Okita K, Iwahashi H, Hanafusa T, and Shimomura I (2010). Expression of chemokines, CXC chemokine ligand 10 (CXCL10) and CXCR3 in the inflamed islets of patients with recent-onset autoimmune type 1 diabetes. Endocr. J 57, 991–996. [PubMed: 20966598]

Wang H, Li J, Zhong P, Wang S, Zhang L, Yang R, Wu D, Chen M, Ji A, Li Y, and Wang J (2019). Blocking CXCR3 with AMG487 ameliorates the blood-retinal barrier disruption in diabetic mice through anti-oxidative. Life Sci. 228, 198–207. [PubMed: 31039363]

Winter WE, and Schatz DA (2011). Autoimmune markers in diabetes. Clin. Chem 57, 168–175. [PubMed: 21127152]

Yamada Y, Okubo Y, Shimada A, Oikawa Y, Yamada S, Narumi S, Matsushima K, and Itoh H (2012). Acceleration of diabetes development in CXC chemokine receptor 3 (CXCR3)-deficient NOD mice. Diabetologia 55, 2238–2245. [PubMed: 22487925]

Yang H, and Yang L (2016). Targeting cAMP/PKA pathway for glycemic control and type 2 diabetes therapy. J. Mol. Endocrinol 57, R93–R108. [PubMed: 27194812]

Zhang X, Goncalves R, and Mosser DM (2008). The isolation and characterization of murine macrophages. Curr. Protoc. Immunol Chapter 14, Unit 14.1.

Zhao Y, Scott NA, Quah HS, Krishnamurthy B, Bond F, Loudovaris T, Mannering SI, Kay TW, and Thomas HE (2015). Mouse pancreatic beta cells express MHC class II and stimulate CD4(+) T cells to proliferate. Eur. J. Immunol 45, 2494–2503. [PubMed: 25959978]

Highlights

- Pro-inflammatory β-cell small extracellular vesicles (cytoEVs) induce β cell dysfunction
- cytoEVs alter the islet transcriptome and enhance leukocyte recruitment to islets
- Pro-inflammatory cytoEV cargo (e.g., CXCL10) activates the CXCL10/CXCR3 axis in β cells
- CXCR3 blockade attenuates cytoEV-mediated β cell dysfunction and leukocyte recruitment

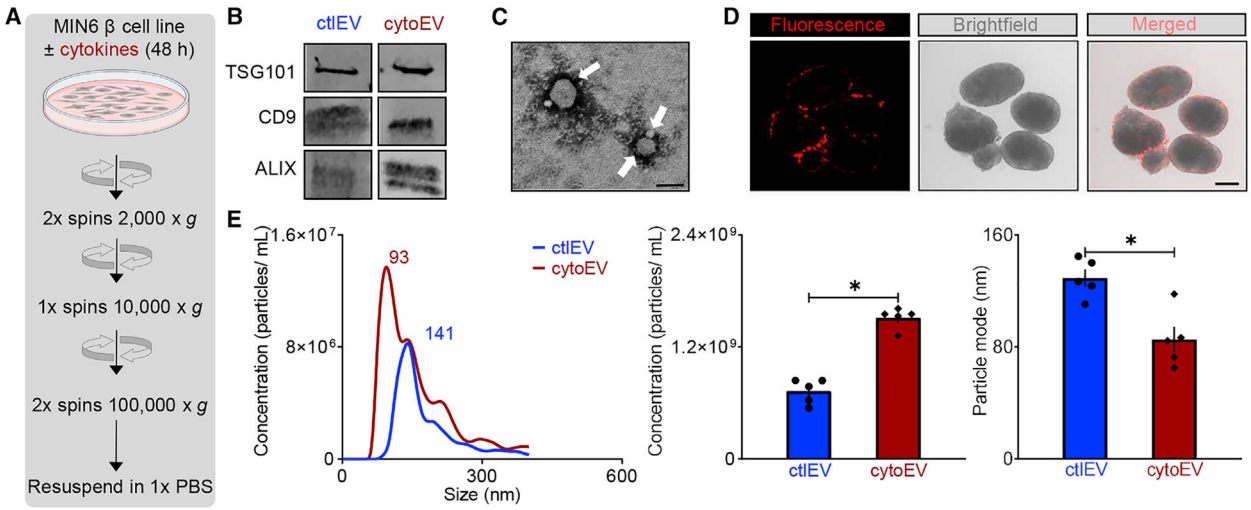

Figure 1. Characterization of cytoEVs

(A) Schematic of our small EV isolation protocol using differential ultracentrifugation for cell culture conditioned medium.

(B) Protein expression of the small EV biogenesis markers TSG101, CD9, and ALIX was identified in isolated MIN6-derived ctlEVs and cytoEVs (representative examples of 2 independent EV isolations).

(C) TEM image of isolated MIN6 small EVs (white arrows, <100 nm). The scale bar represents 100 nm (representative examples of 2 independent EV isolations).

(D) ExoGlow membrane-labeled MIN6 ctlEVs (red; Systems Biosciences) were incubated with isolated mouse islets for 24 h. EV uptake into islets was visualized using confocal microscopy. A representative image was taken from 2 independent experiments using islets isolated from a total of 2 C57BL/6L mice. The scale bar represents 50 μm.

(E) Overlap of representative NTA graphs from MIN6 EVs (untreated, ctlEVs, blue) and cytokine-treated EVs (cytoEVs; red)) with quantification of EV concentrations (particles/mL) in ctlEVs versus cytoEVs and average modal size in 5 independent experiments. Values are mean ± SEM. Statistical significance among groups is indicated by *$p < 0.05$.

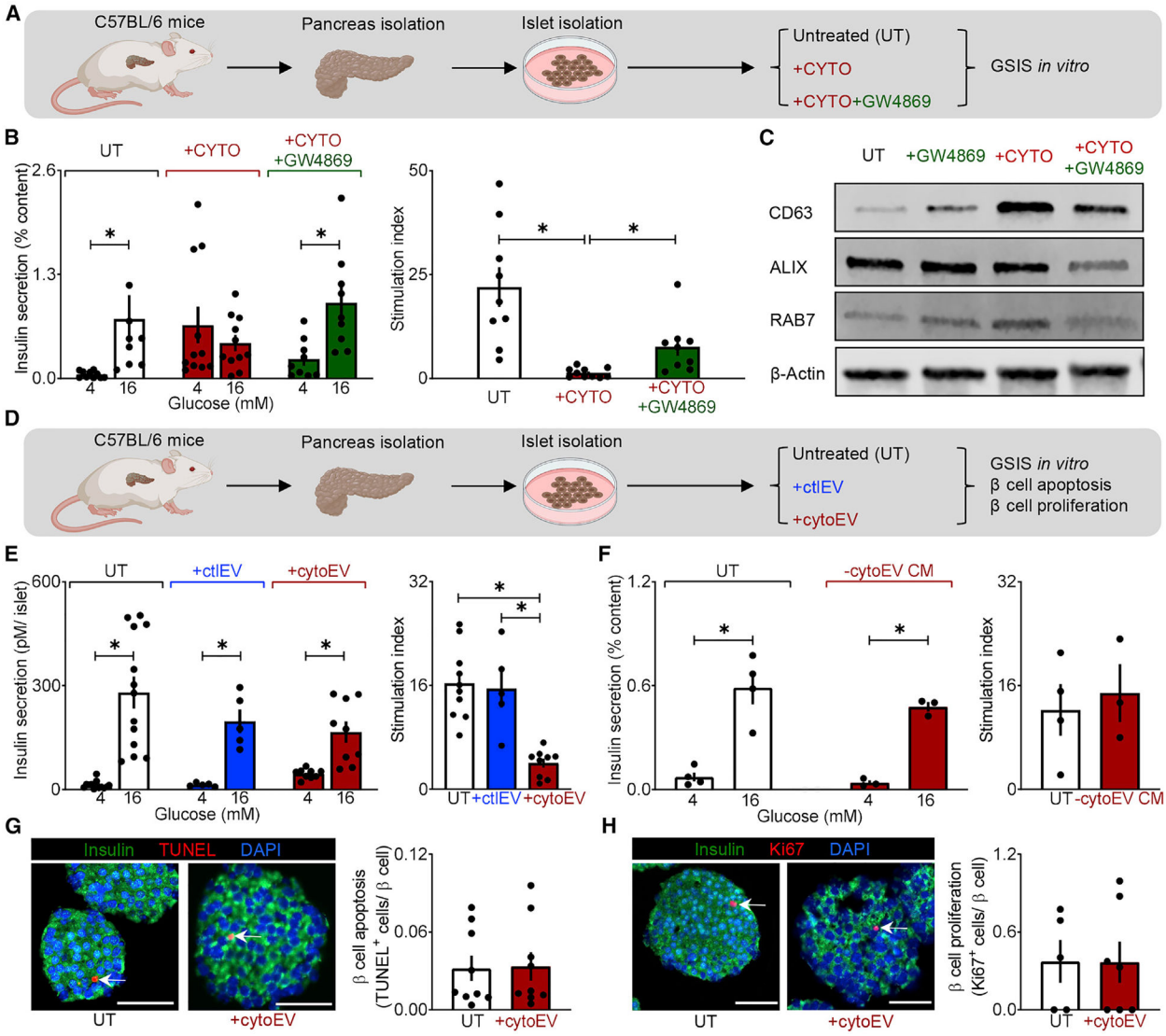

Figure 2. Pro-inflammatory β cell small EVs promote β cell dysfunction in islets

(A) Schematic depicting isolated C57BL/6L mouse islet treatment with CYTO (+CYTO; IL-1β, TNF-α, and IFNγ) or +CYTO+5 μM GW4869 (inhibitor of EV biogenesis) for 24 h, followed by assessment of glucose-stimulated insulin secretion (GSIS).

(B) GSIS assessed by static incubation at 4 mM and 16 mM glucose and corresponding insulin stimulation index (expressed as insulin release during 30 min at hyperglycemic 16 mM glucose over basal 4 mM glucose concentrations) in isolated mouse islets treated for 24 h with CYTO or CYTO+5 μM GW4869 versus untreated (n = 7–9 independent experiments per given condition, with islets isolated from a total of 5 C57BL/6L mice).

(C) Representative protein expression of small EV biogenesis markers in MIN6 cells treated with 5 μM GW4869, CYTO, or combination for 48 h.

(D) Schematic of the experimental design, depicting C57BL/6L mouse islets treated with isolated ctlEVs or cytoEVs for 48 h, followed by assessment of GSIS, β cell apoptosis, and proliferation.

(E) GSIS assessed by static incubation at 4 mM and 16 mM glucose and corresponding insulin stimulation index in isolated mouse islets treated for 48 h with ctlEVs or cytoEVs (treatment of 2×10^9 EVs/day) versus untreated (UT) (n = 5–13 independent experiments per given condition, with islets isolated from a total of 8 C57BL/6L mice).
(F) GSIS assessed by static incubation at 4 mM and 16 mM glucose and corresponding insulin stimulation index in isolated mouse islets treated for 48 h with an equal volume of conditioned medium devoid of cytoEVs versus UT (n = 2–3 independent experiments per given conditions, with islets isolated from a total of 2 C57BL/6L mice).
(G) Representative examples of paraffin-embedded mouse islets treated for 48 h with cytoEVs (2×10^9 EVs/day) versus UT and stained by immunofluorescence for insulin (green), the apoptosis marker TUNEL (red), and DAPI (blue), imaged at 20× (scale bars, 50 μm). Also shown is corresponding quantification of the frequency of β cell apoptosis (assessed by $TUNEL^+$, $insulin^+$ staining) in mouse islets treated for 48 h with cytoEVs versus UT (n = 9 sections, each containing 200–800 β cells, were analyzed, with islets isolated from a total of 8 C57BL/6L mice).
(H) Representative examples of paraffin-embedded mouse islets treated for 48 h with cytoEVs (2×10^9 EVs/day) versus UT and stained by immunofluorescence for insulin (green), the replication marker Ki67 (red), and DAPI (blue), imaged at 20× (scale bars, 50 μm). Also shown is corresponding quantification of the frequency of β cell proliferation (assessed by $Ki67^+$, $insulin^+$ staining) in mouse islets treated for 48 h with cytoEVs versus UT (n = 4–7 sections, each containing 200–300 β cells, were analyzed, with islets isolated from a total of 8 C57BL/6L mice).
Values in all graphs are represented as means ± SEM. Statistical significance among groups is depicted by $*p < 0.05$.

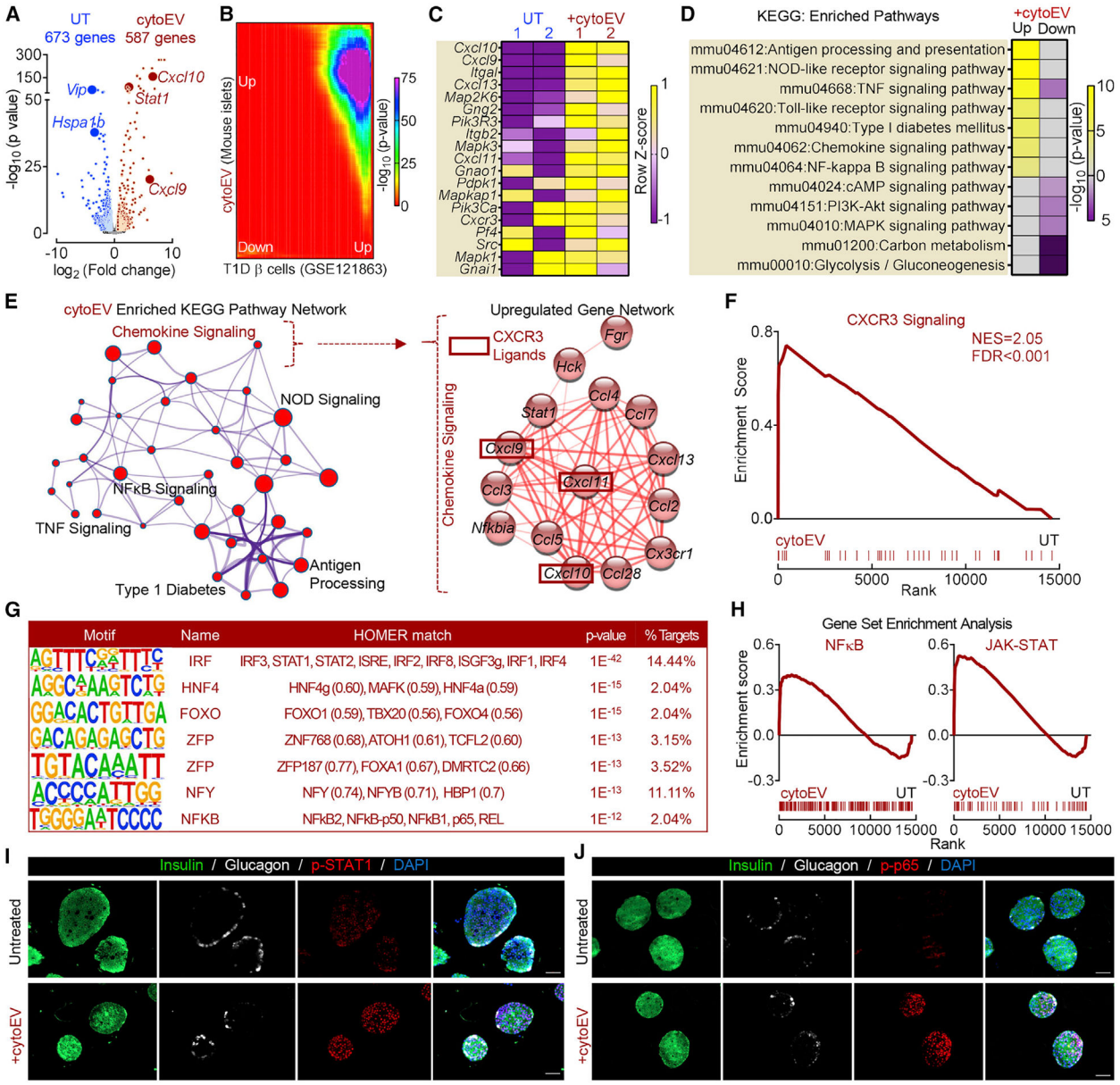

Figure 3. Pro-inflammatory β cell small EVs alter the islet transcriptome

(A) Volcano plot identifying differentially expressed annotated genes (FC > 1.5, $p < 0.05$) from RNA-seq performed on isolated C57BL/6L mouse islets treated for 48 h with cytoEVs (2×10^9 EVs/day) versus UT (n = 2 biological repeats per condition). Note ~600 upregulated and more than 600 downregulated genes with cytoEV addition, with the topmost upregulated/downregulated transcripts (e.g., *Cxcl9*, *Cxcl10*, *Stat1*, *Hspa1b*, and *Vip*) highlighted by enlarged dots (blue and red) on the volcano plot.

(B) Heatmap represents $-\log_{10}$(p value) of rank-rank hypergeometric overlap (RRHO) analysis comparing changes in the islet transcriptome with cytoEV treatment versus the T1D (versus non-diabetic) β cell transcriptome (from GSE121863). Note a significant enrichment ($p < 1 \times 10^{-50}$) in the top right quadrant of the heatmap, depicting the overlap between

upregulated genes in T1D β cells and cytoEV-exposed islets relative to their corresponding controls.

(C) Normalized gene expression depicting top up- and downregulated gene transcripts in mouse islets treated for 48 h with cytoEVs (2×10^9 EVs/day) versus UT. Each column depicts a replicate per condition (n = 2/condition).

(D) KEGG pathway analysis of significantly upregulated and downregulated genes in cytoEV-treated islets versus UT for top up/downregulated KEGG pathways ($p < 0.05$).

(E) *In silico* pathway network analysis illustrating interaction between significantly enriched ($p < 0.05$) KEGG in cytoEV-treated islets versus UT. Key pathways associated with β cell inflammation and dysfunction are highlighted. The size of each node represents the number of gene transcripts associated with each depicted pathway. Of note was the chemokine signaling pathway, which was upregulated because of enrichment of several chemokines, including *Cxcl9*, *Cxcl10*, and *Cxcl11* (boxed in red).

(F) Gene set enrichment analysis (GSEA) performed on a subset of transcripts involved in the CXCR3 pathway (FDR < 0.001) and enriched upon cytoEV treatment in islets (versus UT).

(G) *De novo* motif analysis using hypergeometric optimization of motif enrichment (HOMER) of significantly enriched transcription factor motifs in upregulated genes from islets treated for 48 h with cytoEVs versus UT. The topmost enriched transcription factor motifs in islets upon cytoEV treatment were shown to be associated with pro-inflammatory motifs, including IRF, FOXO, and NF-κB.

(H) GSEA performed on a subset of key genes regulating downstream pathways of NF-κB (FDR = 0.06) and JAK/STAT1 (FDR = 0.02) signaling enriched in isolated islets upon cytoEV treatment (versus UT).

(I) w-κB and STAT1 signaling pathways in islets treated with cytoEVs (versus UT; n = 2 independent experiments per given conditions, with islets isolated from a total of 2 C57BL/6L mice). The scale bars represent 50 μm.

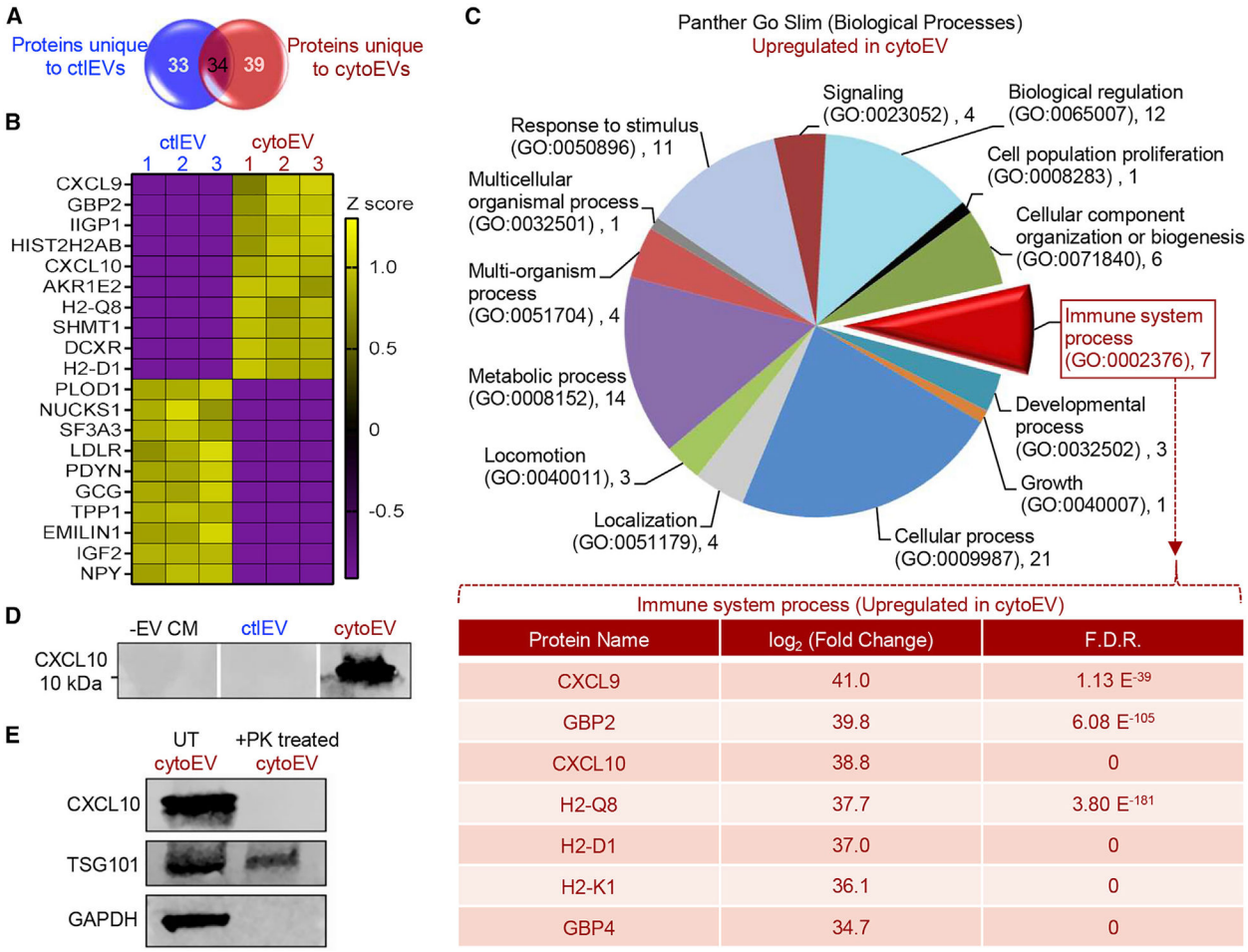

Immune system process (Upregulated in cytoEV)

Protein Name	log_2 (Fold Change)	F.D.R.
CXCL9	41.0	$1.13\ E^{-39}$
GBP2	39.8	$6.08\ E^{-105}$
CXCL10	38.8	0
H2-Q8	37.7	$3.80\ E^{-181}$
H2-D1	37.0	0
H2-K1	36.1	0
GBP4	34.7	0

Figure 4. Proteomic profiling of pro-inflammatory β cell small EVs

(A) Venn diagram depicting the amount of unique and common proteins found in ctlEVs versus cytoEVs isolated from MIN6 cells exposed for 48 h to a combination of pro-inflammatory cytokines (IL-1β [0.2 ng/mL], TNF-α [10 ng/mL], and IFNγ (10 ng/mL]) (cytoEVs) versus (ctlEVs).

(B) Heatmap depicting the top 10 up/downregulated proteins in cytoEVs (versus ctlEVs). CXCL9 and CXCL10 are the most abundant proteins found in cytoEVs. The experiment was completed on 3 independent ctlEV versus cytoEV preparations.

(C) Pie chart depicting the results of Panther GO Slim pathway analysis of proteins significantly enriched in cytoEVs versus ctlEVs. The inset shows several proteins associated with “immune system processes,” which include the top enriched proteins CXCL9 and CXCL10 in cytoEVs.

(D) CXCL10 protein expression assessed by western blotting in cytoEVs and ctlEVs and in medium devoid of cytoEVs after ultracentrifugation (n = 2 independent experiments).

(E) Protein expression of CXCL10, TSG101 (a known intraluminal EV protein), and GAPDH (a known surface EV protein) assessed by western blotting in cytoEVs treated with Proteinase K (PK) versus UT. Lack of CXCL10 expression upon PK treatment indicates membrane-bound topology of CXCL10 in cytoEVs.

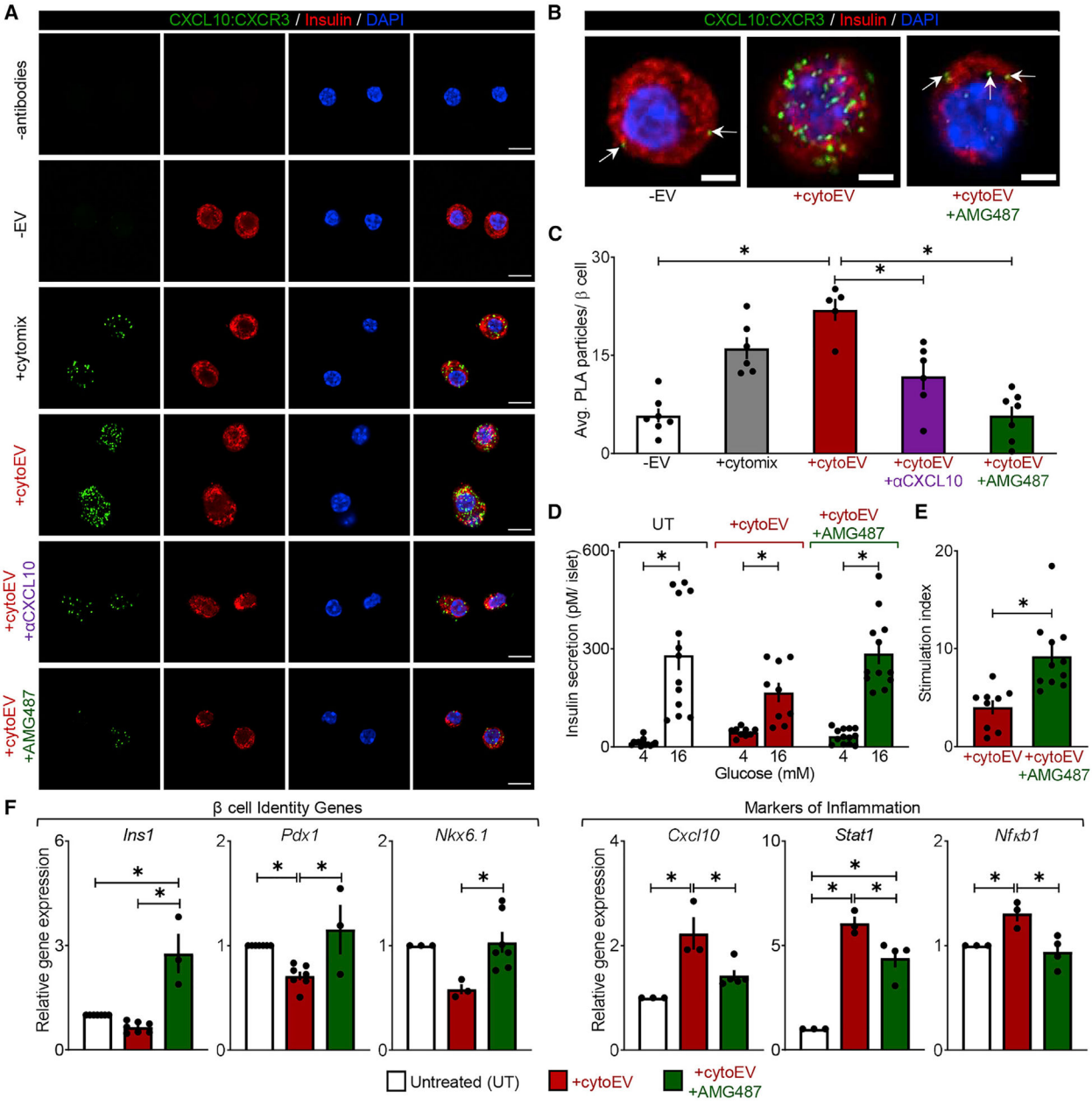

Figure 5. Pro-inflammatory β cell small EVs activate the CXCL10/CXCR3 axis to induce β cell dysfunction

(A) Proximity ligation assay (PLA) was used to determine CXCL10 (ligand):CXCR3(receptor) *in situ* binding. Shown are immunofluorescence images of dispersed mouse islets treated with CYTO, cytoEVs, cytoEV+CXCL10 neutralizing antibody (25 μg/mL), or cytoEV+AMG487 (1 μM, a CXCR3 receptor antagonist) for 48 h versus controls (−EV and –antibodies). Green punctatedots represent CXCL10/CXCR3 interactions, red represents insulin, and DAPI (blue) nuclear stain, imaged at 40× (scale bars, 10 μm).

(B) Representative high-magnification images at 160× (scale bars, 50 μm) of CXCL10/CXCR3 interactions in single β cells treated with cytoEVs or cytoEV+AMG487 for 48 h versus control (−EVs).

(C) Average PLA particles/β cell (CXCL10/CXCR3 interactions) quantified for each condition using ImageJ software (islets were isolated from 3 C57BL/6L mice, and 5–7 independent images containing ~11 β cells/condition were examined).

(D and E) GSIS assessed by static incubation at 4 mM and 16 mM glucose and corresponding insulin stimulation index (expressed as insulin release during 30 min at hyperglycemic 16 mM glucose over basal 4 mM glucose concentration) in isolated mouse islets. Treatments were for 48 h with cytoEVs or cytoEV+AMG487 versus UT (UT and cytoEV data were taken from Figure 2E for comparison; islets were isolated from 3 C57BL/6L mice, with 11 independent experiments for cytoEV+AMG487 treatment). Note restoration of (D) GSIS and (E) stimulation index (~2-fold, green bars).

(F) mRNA expression assessed by qRT-PCR analysis of the β cell identity genes *Ins1*, *Glut2*, and *Pdx1* and the inflammatory genes *Cxcl10*, *Nfκb1*, and *Stat1* in isolated islets treated with cytoEVs or cytoEV+AMG487 versus UT (islets were isolated from 8 C57BL/6L mice, with 2–7 independent experiments per given condition).

All values are a mean ± SEM. Statistical significance among groups is indicated by *$p < 0.05$.

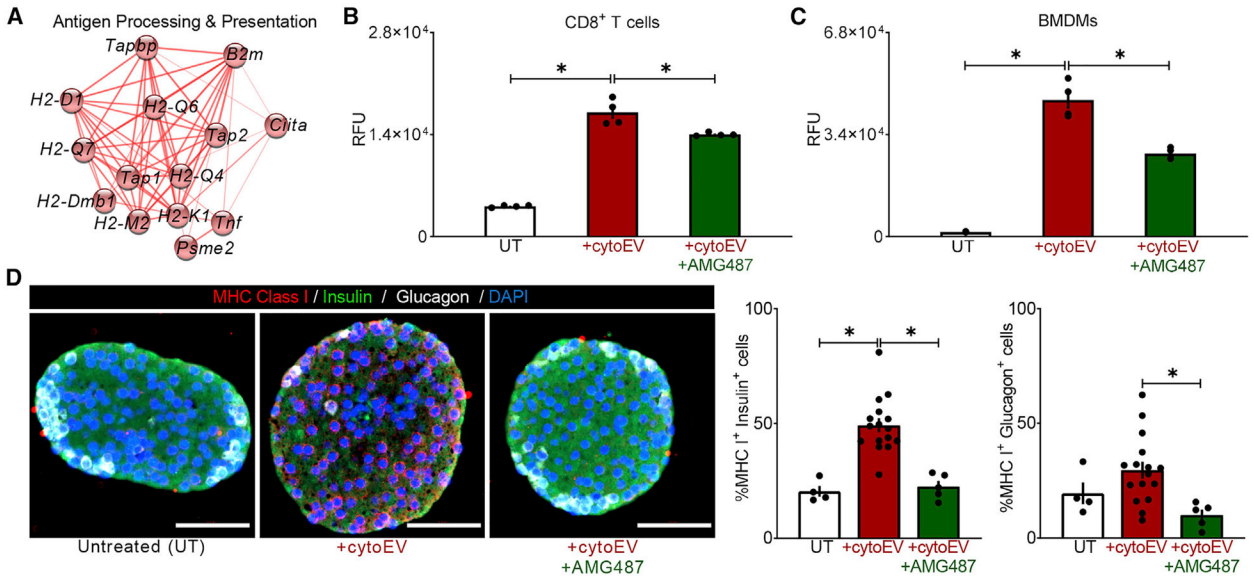

Figure 6. Pro-inflammatory β cell small EVs enhance β cell antigen presentation and immune cell recruitment to islets

(A) Enriched transcripts associated with antigen processing/presentation are depicted in *in silico* network pathway analysis from islets exposed to cytoEVs versus UT.

(B and C) Quantification of migrated $CD8^+$ T cells or bone marrow-derived macrophages (BMDMs) assessed using a chemotaxis assay (relative light units [RFUs]) to isolated mouse islets pre-treated for 24 h with cytoEVs or cytoEV+AMG487 versus UT islets. Isolated $CD8^+$ T cells or BMDMs were incubated with "primed" islets for 8 h (islets were isolated from 2 C57BL/6L mice with 3–4 replicates).

(D) Representative examples of paraffin-embedded and sectioned mouse islets treated for 48 h with cytoEV (2×10^9 EVs/day) versus UT and stained by immunofluorescence for insulin (green), glucagon (white), and MHC class I (red), imaged at 20×. The scale bar represents 50 μm. Also shown is corresponding quantification of β cell and α cell MHC class I expression (assessed by MHC I^+ $insulin^+$/$glucagon^+$ staining) in mouse islets treated for 48 h with cytoEVs or cytoEV+AMG487 (5 μM) versus UT (islets were isolated from 2 C57BL/6L mice, with 3–10 sections analyzed, each containing 5–22 islets).

Values are a mean ± SEM. Statistical significance among groups is indicated by $*p < 0.05$.

KEY RESOURCES TABLE

REAGENT or RESOURCE	SOURCE	IDENTIFIER
Antibodies		
Insulin Antibody, guinea pig polyclonal (IF 1:100)	Abcam	Cat# ab7842; RRID:AB_306130
Phospho-NF-κB p65 (Ser536)(93H1) Antibody, rabbit monoclonal (IF 1:1000)	Cell Signaling	Cat# 3033; RRID:AB_331284
Phospho-Stat1 (Tyr701)(58D6) Antibody, rabbit monoclonal (IF 1:500)	Cell Signaling	Cat# 9167; RRID:AB_561284
HLA ABC Antibody (W6/32), mouse monoclonal (IF 1:100)	Novus Biologicals	Cat# NB100-64775; RRID:AB_2220932
Glucagon Antibody (EP3070), rabbit monoclonal (IF 1:1000)	Abcam	Cat# ab92517; RRID:AB_10561971
CXCL10/IP-10/CRG-2 Antibody, goat polyclonal (IF 1 μg/ml; PLA assay 10 μg/ml)	R&D Systems	Cat# AF-466-NA; RRID:AB_2292487
CD9 Antibody, rabbit polyclonal (WB 1:1000)	System Biosciences	Cat# EXOAB-CD9A-1; RRID:AB_2687469
CXCR3 Antibody, rabbit polyclonal (PLA assay 1:100)	Novus Biologicals	Cat# NB100-56404; RRID:AB_837926
Alix Antibody, rabbit polyclonal (WB 1:1000)	System Biosciences	Cat# EXOAB-ALIX-1; RRID: AB_2892999
MHC Class II (I-A/I-E) antibody, rat monoclonal (IF 1:200)	Invitrogen	Cat# 14-5321-82; RRID:AB_467561
Tsg101 Antibody (C-2), mouse monoclonal (WB 1:500)	Santa Cruz Biotechnology	Cat# sc-7964; RRID:AB_671392
Rab7 (D95F2) Antibody, rabbit monoclonal (WB 1:1000)	Cell Signaling	Cat# 9367; RRID:AB_1904103
Ki67 Antibody Clone B56, mouse monoclonal (IF 1:40)	BD PharMingen	Cat# 550609; RRID:AB_393778
GAPDH Antibody (1D4), mouse monoclonal (WB 1:1000)	Novus Biologicals	Cat# NB300-221; RRID:AB_10077627
Actin Antibody, clone C4, mouse monoclonal (WB 1:5000)	Millipore	Cat# MAB1501; RRID:AB_2223041
IRDye 800CW Donkey anti-Rabbit (WB 1:15,000)	Li-Cor	Cat# 925-32213; RRID:AB_2715510
IRDye 800CW Donkey anti-Guinea Pig (WB 1:15,000)	Li-Cor	Cat# 925-32411; RRID:AB_2814905
IRDye 800CW Donkey anti-Mouse (WB 1:15,000)	Li-Cor	Cat# 925-32212; RRID:AB_2716622
Alexa Fluor® 647 AffiniPure F(ab')2 Fragment Donkey Anti-Guinea Pig (PLA assay 1:100)	Jackson ImmunoReserch	Cat# 706-606-148; RRID:AB_2340477
Chemicals, peptides, and recombinant proteins		
Recombinant Human IL-1β/IL-1F2 Protein	R&D Systems	Cat# 201-LB-005/CF
Recombinant Human TNF-α Protein	R&D Systems	Cat# 210-TA-005/CF
Recombinant Rat IFN-γ Protein	R&D Systems	Cat# 585-IF-100/CF
Vectashield Antifade mounting medium with DAPI	Vector Laboratories	Cat# H-1200-10
SYBR Green Master Mix	ABI	Cat# 4309155
NP40 lysis buffer	Amresco	Cat# J619-500ML
Blotting-Grade Blocker	BioRad	Cat# 1706404
Proteinase K	Promega	Cat# V3021
1X Cell Dissociation Buffer	Sigma	Cat# C5789

REAGENT or RESOURCE	SOURCE	IDENTIFIER
AMG487	MedChemExpress	Cat# HY-15319
Complete macrophage medium w/kit	CellBiologics	Cat# M3368
GW4869	Cayman Chemical	Cat# 13127
Critical commercial assays		
ExoGlow-membrane EV labeling kit	System Biosciences	Cat# EXOGM600A-1
ExoQuick-TC	System Biosciences	Cat# EXOTC10A-1
In Situ Cell Death Detection Kit, TMR red	Roche	Cat# 12156792910
Ultrasensitive mouse insulin ELISA kit	ALPCO	Cat# 80-INSMSU-E10
RNeasy Mini kit	QIAGEN	Cat# 74106
iScript cDNA Synthesis kit	BioRad	Cat# 1708891
EasySep Mouse CD8+ T cell isolation kit	Stem Cell Technologies	Cat# 19853
CytoSelect Chemotaxis Assay kit	Cell Biolabs, Inc	Cat# CBA-102
Bicinchoninic acid (BCA) protein assay	Pierce	Cat# 23227
Deposited data		
RNA-Seq raw and analyzed data	This paper	GEO: GSE175688
Proteomics raw and analyzed data	This paper	PRIDE: PXD026998
Experimental models: Cell lines		
MIN6 cell line	AddexBio	Cat# C0018008
Experimental models: Organisms/strains		
C57BL/6L	Jackson Labs	000664; RRID:IMSR_JAX:000664
Oligonucleotides		
All primers, see Table S1	This paper	N/A
Software and algorithms		
ImageJ	https://imagej.net	RRID:SCR_003070
GraphPad Prism v.6.0d	https://www.graphpad.com:443/	RRID:SCR_002798
ZEN Blue	https://www.zeiss.com/microscopy/en_us/products/microscope-software/zen.html	RRID:SCR_013672
Gene Set Enrichment Analysis (GSEA) 4.0.1	https://www.broadinstitute.org/gsea/	RRID:SCR_003199
HOMER v.4.10	http://homer.ucsd.edu/	RRID:SCR_010881
Rank-Rank Hypergeometric Overlap	https://systems.crump.ucla.edu/rankrank/rankranksimple.php	RRID:SCR_014024
STRING v.11	https://string-db.org/	RRID:SCR_005223
KEGG curated pathways	https://www.kegg.jp/	RRID:SCR_012773
Cytoscape v.3.7.1	https://cytoscape.org/	RRID:SCR_003032
WebGestalt	http://www.webgestalt.org/	RRID:SCR_006786
TopHat v.2.0.6	http://ccb.jhu.edu/software/tophat/index.shtml	RRID:SCR_013035
StringTie v.2.1.3	https://ccb.jhu.edu/software/stringtie/	RRID:SCR_016323
edgeR v.3.1.1	http://bioconductor.org/packages/release/bioc/html/edgeR.html	RRID:SCR_012802
MaxQuant v.1.6.0.1	https://www.biochem.mpg.de/5111795/maxquant	RRID:SCR_014485
PANTHER Gene Ontology	http://www.pantherdb.org/	RRID:SCR_004869